SYNTHESIS OF SILVER NANOPARTICLES USING PEARL MILLET *(PENNISETUM GLAUCUM)* HUSK EXTRACT AND ITS APPLICATION IN WASTEWATER TREATMENT AND CATALYTIC OXIDATION OF BENZYL ALCOHOL

A MINI THESIS SUBMITTED IN PARTIAL FULFILMENT OF THE REQUIREMENTS FOR THE DEGREE OF MASTER OF SCIENCE (CHEMISTRY)

OF

THE UNIVERSITY OF NAMIBIA

BY

PAIDAMOYO SHARON FEKILAH MUSERE

201702663

APRIL 2019

SUPERVISOR: PROF A. RAHMAN (Department of Chemistry and Biochemistry, University of Namibia)

CO-SUPERVISOR: DR V. UAHENGO (Department of Chemistry and Biochemistry, University of Namibia)

Abstract

Metal nanoparticles are endowed with optical, electrical physical and chemical properties and have become attractive materials for commercialization applications in optical spectroscopies, electrical devices and catalytic applications. Among them, silver nanoparticles (Ag-NPs) have distinctive physico-chemical and biological properties such as antimicrobial, chemical stability and catalytic properties. Namibia, a semi-arid country, relies on man-made dams to obtain water for potable use. However, these dams are periodically polluted by algal blooms that pose devastating effects on the water quality. On a separate but related note, there is limited research on the use of Ag-NP based catalysts with regard to the conversion of alcohols to aldehydes as opposed to other noble metals. The aim of this study was to biologically synthesize Ag-NPs and investigate their antimicrobial properties against algae and to further investigate the catalytic properties of Ag-NPs for oxidation of benzyl alcohol. Ag-NPs were formed under optimum conditions. The antimicrobial property of the Ag-NPs was tested by incubating freshwater algae in an Ag-NP solution and the chlorophyll concentration measured periodically. Catalytic properties of Ag-NPs were tested by oxidation of benzyl alcohol in the presence of hydrogen peroxide. The UV-Vis spectroscopic analysis of Ag-NPs revealed a surface plasmon resonance peak at 429 nm. Scanning and transmission electron microscopy showed spherical and polydispersed nanoparticles with an average size of 17 nm. Fourier transform infrared spectroscopy affirmed the role of Pearl Millet extract as a reducing and capping agent of silver ions. Incubation of algae with Ag-NPs resulted in a 41.31% reduction in chlorophyll concentration. High performance liquid chromatography confirmed the oxidation of benzyl alcohol to benzaldehyde, with 90% conversion. The study concluded that biologically synthesized Ag-NPs are toxic to algae and can be used for algae control in wastewater treatment, and furthermore, for catalytic oxidation of benzyl alcohol to form benzaldehyde. The study recommends the use of Ag-NPs as an antimicrobial against algae. In addition, further studies are recommended to investigate the effect of different calcination temperatures and time on the catalytic activity of Ag-NPs.

Conference Proceedings

1. Application of Green Synthesized Silver Nanoparticles: An Environmentally Benevolent Approach in Wastewater Treatment and Catalytic Activity for Benzyl Alcohol Oxidation with Hydrogen Peroxide - Poster presented at the 9th International Conference of the African Materials Research Society, 9-14 December 2017, Gaborone, Botswana.
2. Synthesis Of Silver Nanoparticles Using Pearl Millet *(Pennisetum Glaucum)* Husk And Its Application In Wastewater Treatment And Catalytic Oxidation Of Benzyl Alcohol - Poster presented at the National Students Research Symposium, 18- 19 October 2018, Windhoek, Namibia.

Contents

Abstract i

Conference Proceedings ii

List of tables vii

List of figures vii

List of abbreviations and chemical symbols x

Acknowledgements xi

Dedication xii

Declaration xiii

CHAPTER 1: INTRODUCTION 1

- 1.1 Background of the study 1
- 1.2 Statement of the problem 3
- 1.3 Objectives 4
- 1.4 Significance of the study 4
- 1.5 Limitation of the study 4
- 1.6 Delimitation of the study 4
- 1.7 Outline of thesis 5

CHAPTER 2: LITERATURE REVIEW 6

- 2.1 Introduction 6
- 2.2 Nanotechnology 6
- 2.3 Nanotechnology applications 7
  - 2.3.1. Medicine 7

2.3.2 Agriculture 8

2.3.3 Industry.. 8

2.3.4 Environment 8

2.3.5 Information technology 9

2.4 Synthesis of silver nanoparticles 9

2.4.1 Top to bottom approach..11

2.4.2 Bottom to top approach 11

2.4.3 Photochemical approach 13

2.5 Properties of silver nanoparticles 14

2.5.1 Optical properties..14

2.5.2 Antimicrobial properties 14

2.5.3 Catalytic properties 15

2.5.4 Thermal properties 16

2.5.5 Electrical properties..16

2.6 Eutrophication 16

2.7 Wastewater treatment..20

2.7.1 Methods used to control algae growth..21

2.7.2 Application of Ag-NPs for the control and inhibition of algae growth 27

2.7.3 Disinfection methods used in wastewater treatment 27

2.7.4 Application of silver nanoparticles as a disinfectant in wastewater treatment 31

2.8 Eco-toxicological effects of nanoparticles..31

2.9 Methods of removal of nanoparticles during water treatment 32

2.10 Application of silver nanoparticles in catalysis 32

2.11 Synthesis methods of benzaldehyde 33

2.12 Uses of benzaldehyde 34

CHAPTER 3: METHODOLOGY 35

3.1 Introduction 35

3.2 Research design 35

3.3 Procedures 35

3.3.1 Preparation of pearl millet (*Pennisetum glaucum*) husk extract 35

3.3.2 Synthesis of silver nanoparticles using pearl millet (Pennisetum glaucum) husk extract 36

3.3.3 Determination of optimum conditions for Ag-NP synthesis 37

3.3.4 Characterization of the synthesized silver nanoparticles 38

3.3.5 Collection of algae 40

3.3.6 Exposure of algae to silver nanoparticles 40

3.3.7 Catalytic activity of silver nanoparticles: oxidation of benzyl alcohol to benzaldehyde 41

3.3.8 Energy dispersive x-ray analysis of Ag-NP doped charcoal catalyst 42

3.4 Data analysis 43

CHAPTER 4: RESULTS 44

4.1 Introduction 44

4.2 Determination of optimum conditions for Ag-NP synthesis 44

4.2.1 Effect of pH 44

4.2.2 Effect of silver nitrate concentration 45

4.2.3 Effect of pearl millet extract...45

4.2.4 Effect of temperature 46

4.2.5 Effect of time 47

4.3 Characterisation of Ag-NPs 47

4.3.1 Absorption spectra of Ag-NPs using UV-Vis spectroscopy 47

4.3.2 FT-IR analysis 48

4.3.3 Morphology of Ag-NPs using TEM..49

4.3.4 Morphology of Ag-NPs using SEM 50

4.3.5 Morphology of Ag-NP doped charcoal catalyst using SEM 51

4.3.6 Elemental analysis of Ag-NP doped charcoal catalyst using EDX......................51

4.4 Antimicrobial activity of Ag-NPs on algae 52

4.4.1 Antimicrobial effect of Ag-NPs on chlorophyll concentration in algae 52

4.4.2 Antimicrobial effect of Ag-NPs on algae cell morphology 53

4.5 Catalytic oxidation of benzyl alcohol 54

CHAPTER 5: DISCUSSION 56

5.1 Introduction...56

5.2 Synthesis of silver nanoparticles 56

5.2.1 Effect of pH..57

5.2.2 Effect of silver nitrate concentration 57

5.2.3 Effect of pearl millet extract..58

5.2.4 Effect of temperature 59

5.2.5 Effect of time 60

5.3 Characterisation of Ag-NPs 60

5.3.1 Absorption spectra of Ag-NPs using UV-Vis spectroscopy 60

5.3.2 FT-IR analysis 61

5.3.3 Morphology of Ag-NPs using TEM 61

5.3.4 Morphology of Ag-NPs using SEM 62

5.3.5 Morphology of Ag-NP doped charcoal catalyst using SEM 62

5.3.6 Elemental analysis of Ag-NP doped charcoal catalyst using EDX 62

5.4 Antimicrobial effect of Ag-NPs on chlorophyll concentration in algae 62

5.5 Antimicrobial effect of Ag-NPs on algae cell morphology 64

5.6 Catalytic oxidation of benzyl alcohol 65

CHAPTER 6: CONCLUSION AND RECOMMENDATIONS 67

6.1: Introduction 67

6.2 Conclusions 67

6.3 Recommendations 68

REFERENCES 69

APPENDICES 85

List of tables

Table 1: Harmful freshwater algae, toxins and adverse impacts 18

List of figures

Figure 1: Nanotechnology applications 7

Figure 2: Synthesis techniques of nanoparticles 10

Figure 3: Schematic representation of top to bottom and bottom to top approaches............10

Figure 4: Stages of silver nanoparticle biological synthesis 13

Figure 5: Algae floating along the Swakop river 20

Figure 6: Colour change of water in Swakoppoort dam due to the presence of algae 20

Figure 7: Water stratification 24

Figure 8: Solar bee for algal bloom control 25

Figure 9: Substances removed from water by membrane filtration processes 28

Figure 10: Pearl millet grains 36

Figure 11: Pearl millet husks 36

Figure 12: UV-Vis absorption spectrum of synthesized silver nanoparticles at different pH values 44

Figure 13: UV-Vis absorption spectrum of synthesized silver nanoparticles at varying $AgNO_3$ concentration 45

Figure 14: UV-Vis absorption spectrum of synthesized silver nanoparticles at varying Pearl Millet extract volume 46

Figure 15: UV-Vis absorption spectrum of synthesized silver nanoparticles at different temperatures 46

Figure 16: UV-Vis absorption spectrum of synthesized silver nanoparticles at different times 47

Figure 17: UV-Vis absorption spectrum of silver nanoparticles showing the SPR peak 48

Figure 18: FT-IR spectrum of pearl millet husk and Ag-NPs...49

Figure 19: TEM micrographs of Ag-NPs at 100 nm and 20 nm magnification 49

Figure 20: Particle size distribution of Ag-NPs 50

Figure 21: SEM micrographs showing the morphology of Ag-NPs..................................50

Figure 22: SEM micrographs showing the morphology of Ag-NP doped charcoal 51

Figure 23: EDX spectrum of Ag-NP doped charcoal catalyst 52

Figure 24: Variation in the chlorophyll concentration of algae upon exposure to varying Ag-NPs concentration 53

Figure 25: a. Bright green algae (control), b. Algae exposed to Ag-NPs turning dark green/brown 53

Figure 26: Live Spirogyra algae from literature 54

Figure 27: Live algae from Von Bach dam and Swakop river 54

Figure 28: Dead algae (death due to natural causes) 54

Figure 29: Dead algae exposed to Ag-NPs 54

Figure 30: HPLC chromatogram showing retention time of benzyl alcohol 55

Figure 31: HPLC chromatogram showing retention time of benzaldehyde 55

Figure 32: HPLC chromatogram showing retention time of the reaction mixture product 55

Figure 33: Colour changes during synthesis of Ag-NPs (effect of $AgNO_3$ concentration from 1- 3 mM) 56

Figure 34: Proposed reaction mechanism of catalysis 66

List of abbreviations and chemical symbols

Ag-NPs	Silver Nanoparticles
$AgNO_3$	Silver Nitrate
Ag^+	Silver ion
Ag	Silver
DBPs	Disinfection by-products
EDX	Energy Dispersive X-Ray
FT-IR	Fourier Transform- Infrared
Fe^{2+}	Iron ion
HABs	Harmful Algal Blooms
H_2O_2	Hydrogen Peroxide
O_3	Ozone
PME	Pearl Millet Extract
P	Phosphorus
SEM	Scanning Electron Microscopy
SPR	Surface Plasmon Resonance
TEM	Transmission Electron Microscopy
THMs	Tri-halo Methanes
UV/Vis	Ultra Violet/ Visible

Acknowledgements

To the Author of Life and all that is in it, to Him in which all that finds its purpose and meaning, I say all glory and honour be to God, the ultimate King of kings who always provides for me and paves my way to success. To my beloved family and friends, words can never express how I am deeply grateful for all the support you have given me throughout the course of my studies. I am also humbled to deeply express my heartfelt gratitude for the never ending support from my beloved fiancé S.J Dzimwasha.

I deeply acknowledge the roles played by my supervisor and co-supervisor –Prof Ateeq Rahman and Dr Veikko Uahengo for all the extra push in the right direction and the thorough guidance each day. I would also like to thank the University of KwaZulu-Natal in Durban, South Africa, for their valuable assistance with the use of their analytical instrumentation. Lastly, I extend my sincere gratitude to the University of Namibia, Department of Chemistry and Biochemistry technologists and staff for giving me the opportunity to carry out this research.

Dedication

To my parents, Mr and Mrs Musere, whose unwavered love, support and sacrifices have been the foundation of my academic pursuit.

Declaration

I, Paidamoyo S.F Musere, hereby declare that this study is my own work and is a true reflection of my research, and that this work, or any part thereof has not been submitted for a degree at any other institution.

No part of this thesis may be reproduced, stored in any retrieval system, or transmitted in any form, or by means of electronic, mechanical, photocopying, recording or otherwise without the prior permission of the author, or The University of Namibia in that behalf.

I, Paidamoyo S.F Musere, grant The University of Namibia the right to reproduce this thesis in whole or in part, in any manner or format, which The University of Namibia may deem fit.

………………………………………………	……………………………………	…………………
Name of Student	**Signature**	**Date**

CHAPTER 1: INTRODUCTION

1.1 Background of the study

Nanotechnology is an emerging technology with applications in various fields, such as manufacturing, medicine and healthcare, energy, and information technology industries. It involves the study, production, and manipulation of materials on a scale of 1– 100 nanometres [1]. Synthesis of nanoparticles employs chemical and physical methods, which often have a considerable environmental impact and moreover, technically laborious and expensive. This has led to the development of eco-friendly biological methods as an alternative [2]. Metal nanoparticles, in particular, are endowed with physico-chemical properties such as optical, electrical, antimicrobial, catalytic and magnetic properties [3]. In comparison to other nanomaterials, metal nanoparticles have been proven to be the most flexible nanostructures owing to the synthetic control of their size, shape, composition, structure, assembly, and encapsulation, as well as the resulting tunability of their optical properties [4]. The aim of this study was to synthesize silver nanoparticles (Ag-NPs) by a biological route using Pearl millet (*Pennisetum glaucum*) a drought-resistant grain locally grown in Namibia and popularly known as “Mahangu” [5]. Ag-NPs possess unique antimicrobial and catalytic properties, and for this study, the antimicrobial properties were exploited in wastewater treatment for algae control, whilst the catalytic properties were exploited for catalytic oxidation of benzyl alcohol [2].

Africa is one of the world’s driest continents and is facing a very severe water crisis. Climate change has resulted in increases in temperature and variations in regional precipitation and these changes are expected to intensify in the future [6]. Rapid industrial development, urbanization and population growth have also contributed to water scarcity due to its adverse effects on water quality. Less than 1% freshwater is available for terrestrial and aquatic biota, ecosystems, and human life that depends on it [7]. Therefore, there is a need for recycling water to cater to activities that sustain human, plant and animal life through wastewater treatment [8].

Windhoek, the capital city of Namibia holds the largest population and typically relies on three sources of water for potable use i.e. groundwater (23%), surface water (56%) and recycled water (21%) [9]. Of the three, surface water from man-made dams is a major source for obtaining water for potable use. The Namibia Water Corporation (Namwater) is a bulk potable water distributor and relies on an integrated three-dam system (Von Bach Dam, Swakoppoort Dam and Omatako Dam) to supply treated water to Windhoek and neighbouring towns [10]. These dams are however periodically polluted by algal blooms. In a study conducted by Garus-Oas [11], abundant algae identified was Cyanobacteria such as *Cyanophyceae*, Chlorophyta such as *Chlorophyceae* and Bacillariophyta such as *Aulacoseira*. Cyanobacteria such as *Microcystin* and *Anabaena* were identified in a study done by Sirunda [12]. Studies revealed that Cyanobacteria pose water quality issues in dam water as they are known to produce toxins, foul taste and odour [13]. Algae growth has been a nuisance over the years and at one point, has resulted in the cutting of water supply from Swakoppoort Dam to Von Bach Dam in 2010 due to prevailing eutrophic levels in the Swakoppoort Dam [14]. Algae blooms in these dams are a result of nutrient inflows from, mines, farms, urban areas and treatment plant effluent [11]. Pazvakawambwa [9], also cautioned that, “the water supply security to the Central Area of Namibia will be greatly compromised if Swakoppoort Dam pollution is not controlled, as it is part of the integrated three-dam system supplying the Central Area of Namibia” [9]. With water security at risk due to algal blooms, the inherent antimicrobial properties of Ag-

NPs can thus be explored as a means of preventing algae growth and improving water quality.

On a separate but related note, benzaldehyde is an industrially important aromatic aldehyde, widely used in food, pharmaceutical, cosmetic and plastic industries. Conventionally, benzaldehyde is produced by the hydrolysis of benzyl chloride. Due to the industrial demand and obligation to reduce chlorine-dependent chemical production, the synthesis method in current use is the oxidation of toluene in gas and liquid phase, however, benzoic acid is formed as the main product and benzaldehyde as a by-product [15]. Several noble metals such as platinum, titanium, gold, ruthenium and palladium nanoparticle catalysts have been reported in literature with regard to the conversion of alcohols to aldehydes. However, research on Ag-NP based catalysts has been limited [16]. Ag-NPs nano-porous in nature can be exploited as a catalyst for benzyl alcohol oxidation to the corresponding carbonyl compound. This is, therefore, a fundamental and important transformation in organic chemistry as the product is a valuable synthetic intermediate in various industries.

1.2 Statement of the problem

Namibia is a semi-arid country in Southern Africa, where man-made dams play an important role in obtaining potable water. Algal growth in these dams has posed devastating effects on water quality. Algae affects water quality by producing foul odour and taste and releasing algal toxins. In water treatment processes, it results in clogging of water intake screens and increasing coagulant and disinfection chemical demand [11]. This, in turn, results in costly and cumbersome water treatment processes. Extensive research is therefore required to promote the use of Ag-NPs in Namibia as an antimicrobial for algae control. In addition, a limited number of studies involve the use of green synthesized Ag-NPs for the catalytic oxidation of benzyl alcohol to benzaldehyde [16].

1.3 Objectives

- **a.** To synthesize Ag-NPs using Pearl millet (*Pennisetum glaucum*) husk extract as a reducing agent.
- **b.** To characterise Ag-NPs in terms of their structural and morphological properties, as well as their catalytic activity.
- **c.** To determine the effectiveness of antimicrobial properties of Ag-NPs on algae in Windhoek wastewater.

1.4 Significance of the study

The research will enable the use of green synthesized Ag-NPs as an antimicrobial agent, for use in water bodies for algae control. Furthermore, the knowledge of Ag-NPs' antimicrobial properties in this research can be used to promote their use as a general disinfectant during wastewater treatment to reduce harmful disinfection by-products (DBPs) formed by conventional disinfection methods (e.g. chlorine-based disinfectants). In addition, the research will contribute to studies of green synthesized Ag-NPs as a catalyst for oxidation of benzyl alcohol to benzaldehyde.

1.5 Limitation of the study

The researcher could not access Fourier Transform Infrared (FT-IR) and Gas Chromatography – Mass Spectrometry (GC-MS) for analysis of chemical structures of benzyl alcohol, benzaldehyde and reaction mixture product.

1.6 Delimitation of the study

The study focused on the application of green synthesized Ag-NPs on Windhoek wastewater treatment for algae inhibition and catalytic activity for benzyl alcohol oxidation.

1.7 Outline of thesis

The study consists of six chapters as described below:

- Chapter One gives a background of the research, problem statement, objectives and the justification of the study.
- Chapter Two reviews the work done by other researchers. This is presented in the form of a comprehensive literature review on the application of nanotechnology in various fields, synthesis methods of Ag-NPs and properties of Ag-NPs that make them viable for application as an antimicrobial and catalyst.
- Chapter Three presents the methods used for data collection and analysis and procedures for experimental work carried out.
- Chapter Four presents the results obtained from the experimental work done as outlined in Chapter Three.
- Chapter Five interprets the results obtained and intensely explains the relation to the theoretical body of knowledge on the topic.
- Chapter Six gives conclusions drawn from the discussion of the results, it goes further to give recommendations.

CHAPTER 2: LITERATURE REVIEW

2.1 Introduction

This chapter reviewed the literature on nanotechnology and its applications. The use of nanotechnology was narrowed down to metal nanoparticles (silver). This was followed by a review of the synthesis methods of Ag-NPs and their properties that make them viable for application as an antimicrobial agent and as a catalyst. The review went further to look into eutrophication, its effects, methods of control and potential use of Ag-NPs to control the effects of eutrophication. Current wastewater disinfection methods and potential use of Ag-NPs as a disinfectant were reviewed. Lastly, application of Ag-NPs in catalysis, synthesis methods, and uses of benzaldehyde were reviewed.

2.2 Nanotechnology

Nanotechnology involves the study of the fundamental aspects of physics, chemistry, biology and technology of materials on a nanometre-scale [17]. Nanotechnology has resulted in breakthroughs in areas such as materials and manufacturing, medicine and healthcare, energy, biotechnology, environmental science and information technology [17]. The history of nanotechnology dates back to the 29th of December 1959, when at the California Institute of Technology, Nobel Prize Laureate Richard P. Feynman gave a famous lecture at the Annual Meeting of the American Physical Society, entitled: There’s Plenty of Room at the Bottom [18]. He presented a technological vision of extreme miniaturization where he spoke about the manipulation and control of objects on a small scale. Since the 1980s, many inventions and discoveries in the fabrication of nano-objects have been a result of his vision [17].

2.3 Nanotechnology applications

The world has experienced an exponential growth in the application of nanotechnology, leading to great strides in the development of new nanomaterials. The increase in innovation is largely due to the special properties that these materials possess at the nanoscale, such as mechanical and physico-chemical properties [19]. Nanotechnology finds its application in commercial and technological fields and is believed to be the next Industrial Revolution. The main nanotechnology applications are shown in Figure 1 below:

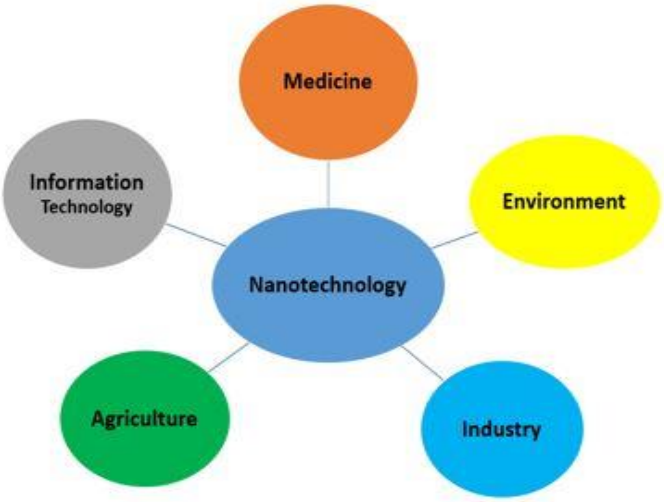

Figure 1: Nanotechnology applications **[20]**

2.3.1. Medicine

In medicine, nanoparticles are employed for various applications, among them drug delivery and cell repair to diseased cells, which allows direct treatment of those cells. Nanoparticles can be used for therapy techniques such as chemo-therapy whereby concentrated radiation is used to treat cancer tumours without damaging healthy cells. Nanoparticles are also used for diagnostic techniques for earlier detection of diseases. Lastly, nanoparticles have been incorporated into medical antimicrobial techniques to improve cleaning of instruments in hospital settings and to treat antibiotic-resistant infections [21].

2.3.2 Agriculture

The use of nanotechnology in agriculture is relatively new and research is focusing on the use of nano-capsules and nanoparticles for the detection and treatment of diseases, the enhancement of nutrients absorption by plants and the delivery of active ingredients to specific parts of a plant [22]. The use of target-specific nanoparticles can reduce the damage to non-target plant tissues and control the amount of chemicals released into the environment. Recently, nano-sensors have found application in agriculture due to their strengths in environmental monitoring of contamination in soil and water [23].

2.3.3 Industry

Nanotechnology has found use in various industries such as manufacturing industries. Nanoparticles can be used as catalysts to enable complex chemical reactions to occur at lower temperatures thus making reactions more efficient and safe. Nanotechnology is currently being applied to make batteries that are quicker-charging, efficient, lighter weight, have a higher power density, and hold electrical charge longer and lastly incorporation into solar panels to convert sunlight to electricity more efficiently [24].

2.3.4 Environment

Nanotechnology has enabled the development of sensors to detect very small amounts of chemical vapours or molecules within the environment. Carbon nanotubes can be used for air quality monitoring stations to improve the tracking of air pollution sources [25]. Nanotechnology can also be applied in the control of water pollution by use of nanoscavengers that act as antimicrobial agents or photo-catalysts that have the ability to break down organic contaminants and or trap heavy metal pollutants present in water [26].

2.3.5 Information technology

Nanotechnology has contributed immensely in computing and electronics, by producing faster, smaller, and more portable systems that can manage and store large amounts of information. Nanoparticle copper suspensions have also been developed as a safer alternative to lead-based solder and other hazardous materials commonly used to fuse electronics during assembly [24].

2.4 Synthesis of silver nanoparticles

Among the several noble metal nanoparticles, silver nanoparticles (Ag-NPs) have attracted special attention due to their unique structures, size and their distinct physical, chemical and biological properties as compared to their bulk counterparts [20]. Ag-NPs have distinctive physico-chemical properties, such as high electrical and thermal conductivity, surface-enhanced Raman scattering, chemical stability, catalytic activity and nonlinear optical behaviour. Furthermore, Ag-NPs exhibit broad-spectrum bactericidal and fungicidal activity [1]. Synthesis methods employ two approaches which are illustrated in Figure 2 and 3 below:

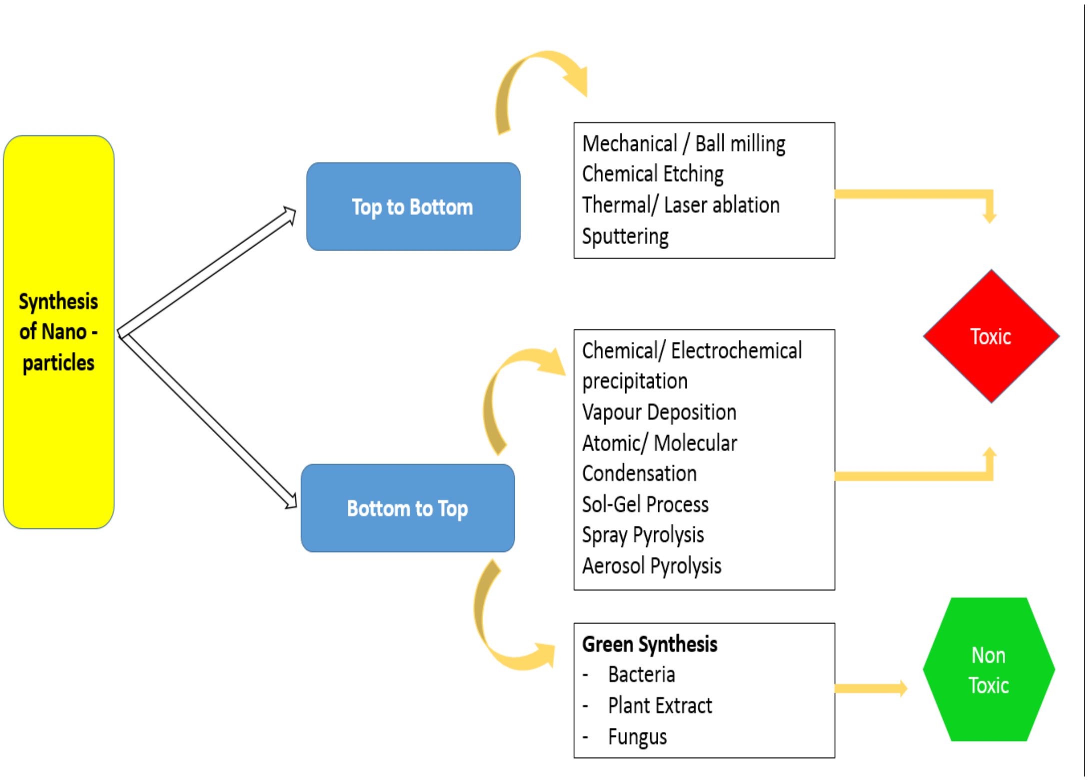

Figure 2: Synthesis techniques of nanoparticles [27]

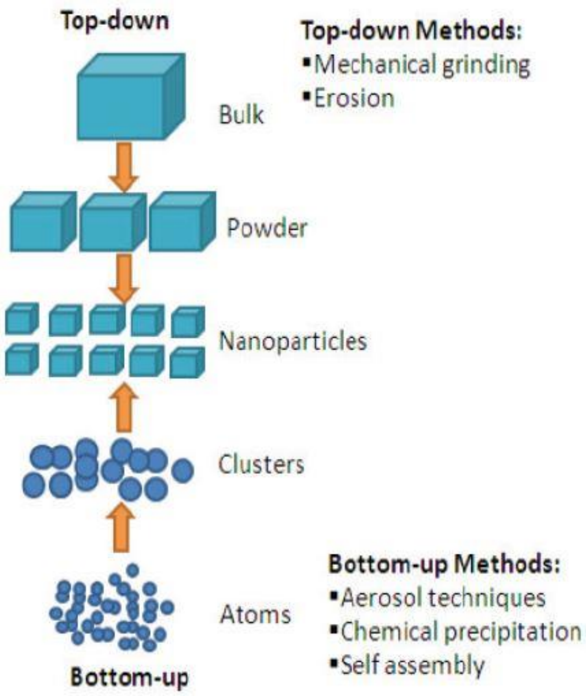

Figure 3: Schematic representation of top to bottom and bottom to top approaches [28]

2.4.1 Top to bottom approach

In the top to bottom approach, the size of the silver metal in its bulk form reduces mechanically to the nano-scale by using physical methods such as evaporation-condensation, laser ablation, ball milling and chemical etching [29].

i. Physical synthesis

Physical synthesis methods involve the use of mechanical pressure, high energy radiations, thermal energy or electrical energy to cause material abrasion, melting and evaporation-condensation to synthesize nanoparticles [30]. Ball milling, laser ablation, electrospraying, inert gas condensation, physical vapour deposition are some of the most regularly used physical methods to synthesize nanoparticles. The major drawbacks of this synthesis method are that it requires a large amount of energy while raising the environmental temperature around the source material, it requires a lot of time to achieve thermal stability and lastly, a large space is required to set up the system [1]. The physical approach, however, permits the production of large quantities of Ag-NPs samples in a single process and is also a useful method to produce Ag-NPs in powder form [1].

2.4.2 Bottom to top approach

The bottom to top approach is a self-assembly technique and includes dissolution of silver salt into a solvent, reduction of silver ions to their element using the addition of a reducing agent and then stabilization of the forming Ag-NPs using a stabilizing agent to prevent agglomeration of nanoparticles [29]. This approach employs two synthesis methods.

i. Chemical synthesis

In chemical synthesis, the chemical reduction method is used for the synthesis of nanoparticles. Silver salts are reduced by a chemical reducing agent by forming a silver nucleus and the growth of the nucleus to a particle controlled by a capping agent which prevents aggregation by steric hindrance or electrostatic repulsion [2]. Various organic and inorganic reducing agents, such as sodium borohydride, sodium citrate, ascorbate, elemental hydrogen, Tollen's reagent, N,N-dimethyl formamide and poly (ethylene glycol) block copolymers are used for reduction of silver ions (Ag^+) in aqueous or non-aqueous solutions. Chemical reduction methods used are pyrolysis, inert gas condensation, solvothermal reaction, sol-gel fabrication and microemulsion solutions [27]. However, chemical synthesis methods use toxic chemicals, which are hazardous to the environment and result in the adsorption of toxic chemicals on to the surface of synthesized Ag-NPs, making them unsuitable for biomedical applications [2].

ii. Biological synthesis

The need for the development of environmentally conscious, cost-effective and energy-efficient synthesis methods that avoid toxic and hazardous chemicals has resulted in the development of biological (green) synthesis of Ag-NPs using plants, microorganisms and biopolymers [31], [32].

Biomolecules existing in plant extracts are enzymes, proteins, amino acids, vitamins, polysaccharides, organic acids, terpenoids, polyphenols, sugars, alkaloids and phenolic acids [29]. All the above-mentioned extract compositions take part in Ag-NP synthesis by reducing and capping. The exact mechanism is not known however it is suggested that the metal ion Ag^+ is reduced to Ag^0 by active biomolecules such as phenolic compounds [20], this is followed by nanoparticle growth and stabilisation to avoid agglomeration, this is shown in Figure 4 below:

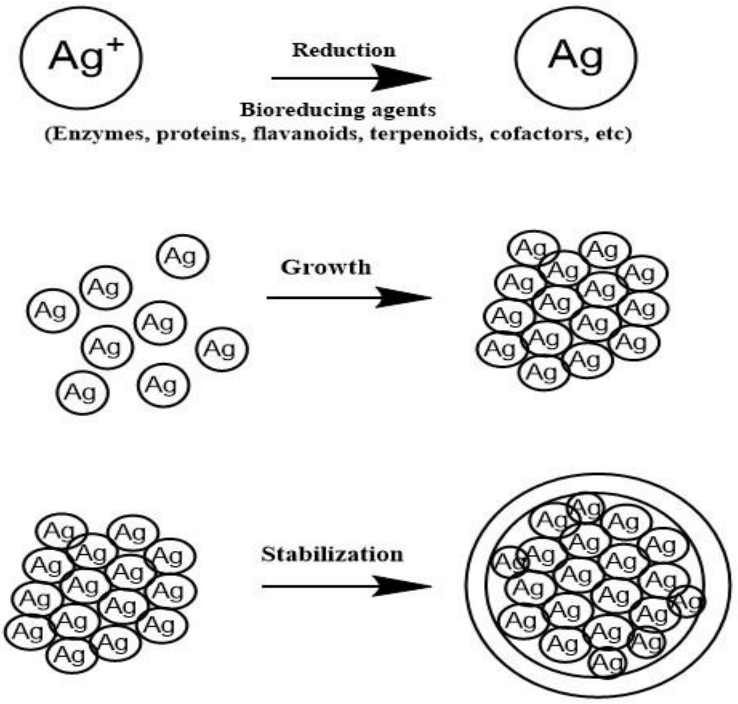

Figure 4: Stages of silver nanoparticle biological synthesis **[29]**

Plants have been noted to be better synthesizers as compared to the other biological methods due to the abundance of plant resources. Additionally, the use of plant extracts is cheaper as compared to the cost of microorganism isolation and culture media for nanoparticle synthesis using microorganisms [33].

2.4.3 Photochemical approach

Photochemical synthesis is now being considered as an alternative method for obtaining colloidal nanoparticles. The photo-induced synthetic strategy is categorized into two distinct approaches, that is the photo-physical (top to bottom) and photochemical (bottom to top). The nanoparticles are formed by the direct photo-reduction of a metal source or reduction of metal ions using photo-chemically generated intermediates, such as excited molecules and radicals, this is often called photosensitization [34].

2.5 Properties of silver nanoparticles

Ag-NPs, among all other metals, have been investigated because of their unique optical, biological, electronic and chemical properties that depend on their shape and sizes [35].

2.5.1 Optical properties

Ag-NPs are efficient at absorbing and scattering light. When exposed to light at a specific wavelength, the oscillating electromagnetic field of the light induces a collective coherent oscillation of the free electrons on the metal surface, which causes a charge separation, forming a dipole oscillation along the direction of the electric field of the light. The amplitude of the oscillation reaches a maximum at a specific frequency, called Surface Plasmon Resonance (SPR) [36]**.** Optical properties of Ag-NPs have the potential use in sensor devices. Recently, their optical properties have been capitalized for their use as sensors for sensitive colourimetric detection of chromium in surface waters and industrial wastewater [37]. Ag-NPs unique optical property is also in use for light harvesting in solar cells, enhanced optical spectroscopies such as metal-enhanced fluorescence and surface-enhanced Raman scattering by improving signal intensity [38].

2.5.2 Antimicrobial properties

Ag-NPs possess antimicrobial properties. This is also known as the Oligodynamic effect (from Greek terminology, oligos meaning "few", and dynamis meaning "force"), which is the ability of small amounts of heavy metals to exert a toxic effect on bacterial cells. This action of metals and metal compounds was noted in 1893 by Carl Wilhelm von Naegeli a Swiss botanist who pointed out that, “definite metals and metal compounds confer in a minute quantity of water solutions the ability to change and finally kill cells of microorganisms in a ‘characteristic way’,” [39]. This antimicrobial effect is shown by metals such as mercury, silver, copper, lead, zinc, gold and aluminium among other metals [40].

The exact mechanism of the antimicrobial action is still unknown, thus is an area of dynamic research, however, it has been hypothesised that the metal ions denature enzymes of the target cell or organism by binding to reactive groups, resulting in their precipitation and inactivation [41]. Out of all the metals with antimicrobial properties, it was discovered that silver has the most effective antimicrobial action and is least toxic to animal cells [27]. However excessive exposure to silver in humans, if consumed in large quantities leads to a permanent change in skin colour to blue-grey, a condition known as Argyria [42].

Silver has an antimicrobial effect on approximately 650 types of diseases causing microorganisms. Silver inactivates enzymes by reacting with the amino-, carboxyl-, phosphate-, and imidazole-groups and diminishes the activity of key enzymes that are necessary for the metabolic activities of the bacteria [43]. Ag-NPs antimicrobial activity is more pronounced against Gram-negative bacteria than Gram-positive bacteria. This is because Gram-negative bacteria have very thin cell walls of peptidoglycan, whereas Gram-positive bacterial cell walls have thick layers of peptidoglycan. Due to thin cell walls of Gram-negative bacteria, the Ag-NPs can penetrate the cell much easier, disrupting the cell wall and increasing cell membrane permeability leading to osmotic collapse [44].

2.5.3 Catalytic properties

The size and shape of silver nanomaterials influence their role in catalysis. Nano-catalysis has attained great interest due to the high surface to volume ratio, and a large number of active sites on the surface of nanoparticles which play a significant role for catalysis [45]. The advantages of Ag-NPs in catalysis are that they are insoluble in the reaction, have high dispersion and allow easy separation of catalyst for recyclability like heterogeneous catalysts.

2.5.4 Thermal properties

Metal nanoparticles exhibit low melting temperature due to the thermodynamic size effect. Studies have investigated the melting points of Ag-NPs having sizes ranging from 4 to 50 nm and have observed that when the size of Ag-NPs decreases, melting occurs at lower temperatures[46]. With this property, Ag-NPs have the potential to be exploited in electrical devices [46].

2.5.5 Electrical properties

Silver has the highest electrical conductivity of all metals [47]. Recently inkjet technology has been used to produce flexible electronic circuits. Ag-NPs have found the use for producing electronic circuits because of the uniformity of the small metal particles dispersed in the inks and their high electrical conductivity [48]. Furthermore, the high electrical conductivity of Ag-NPs has resulted in the interest of the deposition of conductive patterns on substrates like paper, plastic or textile for the fabrication of electronic devices such as chemical sensors and field effect transistors [49].

2.6 Eutrophication

Eutrophication is a natural process that occurs over geological time scales, it results in the enrichment of nutrients in water bodies. It is characterized by excessive plant and algal growth due to the increased availability of limiting growth factors required for photosynthesis such as sunlight, carbon dioxide, and nutrients [50]. Over the past century, due to industrialisation, eutrophication in water bodies has significantly escalated. Eutrophic environments exist naturally, but however commonly results from anthropogenic changes including catchment disturbance and nutrients entering waterways via overland runoff, stormwater and sewage works. With population growth, water usage rises and eutrophication of surface waters can be expected to increase too [51].

Eutrophication creates dense blooms of foul-smelling phytoplankton that reduce water clarity and quality. These blooms rapidly deplete nutrients, increase turbidity and deplete inorganic carbon supplies. Blooms eventually die off, and this is referred to as a “crash”. Following the “crash”, microbial decomposition results and severely depletes dissolved oxygen, creating hypoxic or anoxic conditions which cannot support most aquatic organisms thus leading to large-scale fish mortalities [52]. Anoxic bottom waters promote the sediment release of soluble iron (Fe) and manganese (Mn), causing taste and odour problems in drinking water, as well as the release of hydrogen sulfide (H_2S) and soluble phosphorus (P). Soluble P released from anoxic sediments can become available again for algal uptake resulting in new bloom formation. Furthermore, eutrophication results in depletion of dissolved inorganic carbon and raises pH to extreme levels during the day [52]. Elevated pH can “blind” organisms that rely on dissolved chemicals for their survival by impairing their chemosensory abilities. Lastly, in wastewater treatment, the presence of algae and high loads of organic detritus react with chlorine to form DBPs and clog pipes during treatment [13].

Algal blooms can either be toxic or non-toxic. Over the past decades, coastal regions and freshwaters throughout the world have experienced an escalation in the incidence of toxic blooms known as Harmful Algal Blooms (HABs). Algal blooms that do not produce toxins are also classified as HABs, because most species are able to cause harm through the development of high biomass, leading to algal scums, the depletion of oxygen as they decay and the destruction of habitats for fish or shellfish by shading of submerged vegetation [53]. Algal blooms that commonly release toxins are cyanobacteria, golden algae, diatoms and euglena. However, cyanobacteria blooms are the most prolific and problematic algae. Table 1 below shows the effects of various types of algal toxins:

Table 1: Harmful freshwater algae, toxins and adverse impacts **[54]**

Harmful Algal Blooms (HAB) Taxa	**Toxins**	**Adverse Impacts**
Cyanobacteria	Hepatotoxins, neurotoxins, cytotoxins, dermatotoxins, respiratory and olfactory irritant toxins	Water discolouration, foul-smelling scum, hypoxia from high biomass blooms, taste and odour in drinking water and in farm-raised fish. Dermatitis in humans
Haptophytes (i.e. *Prymnesium parvum*, *Chrysochromulina polylepis*)	Ichthyotoxins	Fish mortality and other gill breathing species.
Chlorophytes Microalgae (*Volvox, Pandorina)*	None	Discolouration of water, localized hypoxia.
Macroalgae (*Cladophora*)	None	Unsightly and foul-smelling mats, localized hypoxia, clogged water intakes during water treatment.
Euglenophytes (*Euglena sanguinea)*	Ichthyotoxins	Discolouration of water and fish mortality.
Raphidophytes (*Chattonella, Heterosigma akashiwo*)	Ichthyotoxins	Fish Mortality
Dinoflagellates (*Alexandrium spp*)	Saxitoxins	Marine mammal mortality

Cryptophytes	None	High biomass blooms can cause discoloured water, localized hypoxia
Diatom (*Didymosphenia geminata*)	None	Produces large amounts of extracellular stalk material resulting in ecosystem and economic impacts.

In Namibia, Windhoek, freshwater man-made dams; Von Bach, Swakoppoort and Goreangab dams are susceptible to eutrophication. The presence of algal blooms in 2010 resulted in the cut-off of water supply from Swakoppoort Dam. A study by Lehmann indicated that the continual presence of algae in Swakoppoort dam may render it “unfit” as a drinking water source or make it expensively difficult to treat [14]. Since 2009, the Goreangab Dams’ water was deemed not fit to be used as a source of water for potable use. With global warming on the rise, Windhoek is at risk of water supply insecurity and this in turn may have an impact on the economy as Windhoek is Namibia’s hub for commercial, industrial, government services, transport, and tourism sectors. This, therefore, prompts the need to control algae growth within the dams [9]. Figures 5 and 6 below show the state of some Windhoek potable water sources:

Figure 5: Algae floating along the Swakop river [Author]

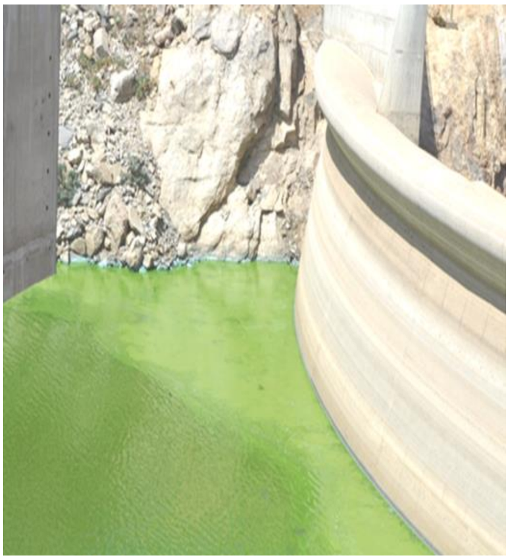

Figure 6: Colour change of water in Swakoppoort dam due to the presence of algae **[55]**

2.7 Wastewater treatment

Water is at the core of sustainable development and is critical for socio-economic development, energy and food production, healthy ecosystems and for human survival. However, with the increase in the global population growth, there is an increasing demand for water and hence the need to balance the competing commercial demands on water resources so that communities have enough for their needs [8].

Human activities that use water, in turn, produce wastewater. With the increase in demand for water, the quantity of wastewater produced is increased as well as its pollution load [8]. Furthermore, the majority of wastewater is released directly to the environment without adequate treatment, resulting in detrimental impacts on human health, the quality of ambient freshwater resources, and ecosystems by mostly producing HABs [8]. Wastewater treatment, therefore, involves applying technology to improve the quality of wastewater, through physical, biological and chemical treatment methods [56].

Methods that have been studied and shown to be useful for the control and growth of algae are discussed in this section. The use of Ag-NPs for algae control and inhibition is also discussed. Lastly, due to disinfection being a very important step in wastewater treatment, common disinfection methods and the use of Ag-NPs as a disinfectant in wastewater treatment are discussed.

2.7.1 Methods used to control algae growth

Algae control methods are divided into nutrient management, physical, chemical and biological methods. These are explained below:

2.7.1.1 Nutrient management

The major nutrient sources are usually from the catchment area. Managing catchment areas to reduce the external load on water reservoirs is crucial but very complex and also not eliminate algal blooms. Strategies to reduce nutrient export and retain P in the catchment include removal of point source contributions such as sewage effluent and intensive agriculture, stormwater management, regulating animal stocking practices, protecting streams with buffer strips, soil treatment with gypsum which binds with P and lastly optimising fertiliser application so as not to over-apply fertilisers. These methods if applied strictly, they can play a role in reducing the nutrient load in lakes and dams [57].

2.7.1.2 Chemical methods

i. Pre-oxidation

Pre-oxidation aids in improving the removal of algal cells by conventional wastewater treatment methods such as coagulation and flocculation. Pre-oxidation chemicals are; ozone, chlorine, chlorine dioxide and potassium permanganate. The effects of disinfection and inactivation of the algae cells cause the changes of the zeta potential to promote their aggregation during further treatment by coagulation. Pre-oxidation by potassium permanganate generates manganese dioxides in situ, which can adhere to the cells and promote their settling. However, pre-oxidation by chlorine or chlorine dioxide forms undesirable DBPs. Ozone, chlorine and potassium permanganate can induce the release of algal toxins through cell lysis which may not be removed by conventional wastewater treatment processes [58].

ii. Clay flocculation

Removal of algae by use of clay flocculants is achieved through rapid flocculation from the interaction of clay particles and algal cells, the entrainment of algal cells into settling clay flocs, and the loss of algal cell motility due to physico-chemical interactions with the clay particles. Floc (algal cells trapped among clay particles), accumulates and settles quickly at the bottom of the water column [59]. Clay flocculants have the advantages of availability, low cost and ease of use. The efficiency depends on the type and amount of clay and may vary depending on the algae species. Common clay flocculants that have been reported are red clay, montmorillonite, kaolin and kaolinite [60].

In addition, modified clays have been developed with the aim to reduce P available in the water. Lanthanum modified bentonite trademarked as ‘Phoslock’ was developed with the aim of dephosphatising the water column and reducing the release of P from a lakes’ sediment. Phoslock is applied as a suspension to the water surface. It removes soluble reactive P from the water by binding with it, and this inhibits the growth of algal blooms [61]. Concerns have however been expressed regarding toxicity to benthic organisms such as snails and mussels whose habitat is affected by the settling floc. Some studies also indicate lanthanum can be bioavailable and can be taken up by marbled crayfish [61].

iii. Algaecides

Algaecides can control algal blooms when used correctly. Commonly used algaecides are copper based (copper sulphates and copper chelates) and hydrogen peroxide (H_2O_2). Chemical methods are regarded to be economical and fast acting, but however, have a higher likelihood of toxicity and non-target response than other available methods. Algaecides vary in their mechanism of action, but they are considered "contact" pesticides, as they cause damage to only the algal cells they come in contact with. They can be sprayed or injected directly into the water column or applied as granular crystals or pellets [57].

The effectiveness of copper-algaecide toxicity is a function of water chemistry, particularly pH, water hardness and dissolved organic content, all of which influence the complexation of the metal to the algae [57]. Copper is one of the metals that possesses the oligodynamic effect as explained in section 2.5.2 Copper affects the electron transport in the photosystem and modifies or inhibits fundamental enzymatic activities within the algal cells thus prompting death [58]. However the continuous use of copper-based algaecides may result in an accumulation of copper in sediments and, consequently, may restrict sediment reuse and disposal.

On the other hand H_2O_2 is a strong oxidizing agent and environmentally friendly. H_2O_2 under light radiation produces highly reactive hydroxyl radicals which cause oxidative damage to cell membranes and inhibits the photosynthesis activity by blocking photosynthetic electron transfer resulting in algal cell death [62]. Due to the high oxidising ability, H_2O_2 may cause damages to the cell structure and thus release toxins into the water. Furthermore, H_2O_2 degrades quickly and should be dosed regularly to ensure consistent control of blooms [63].

2.7.1.3 Physical Methods

i. Water circulation

Water circulation in a reservoir is for destratification, whereby water is mixed to eliminate stratified layers (Epilimnion, Thermocline and Hypolimnion) to make it less favourable for algae growth in certain layers. This is shown in Figure 7 below:

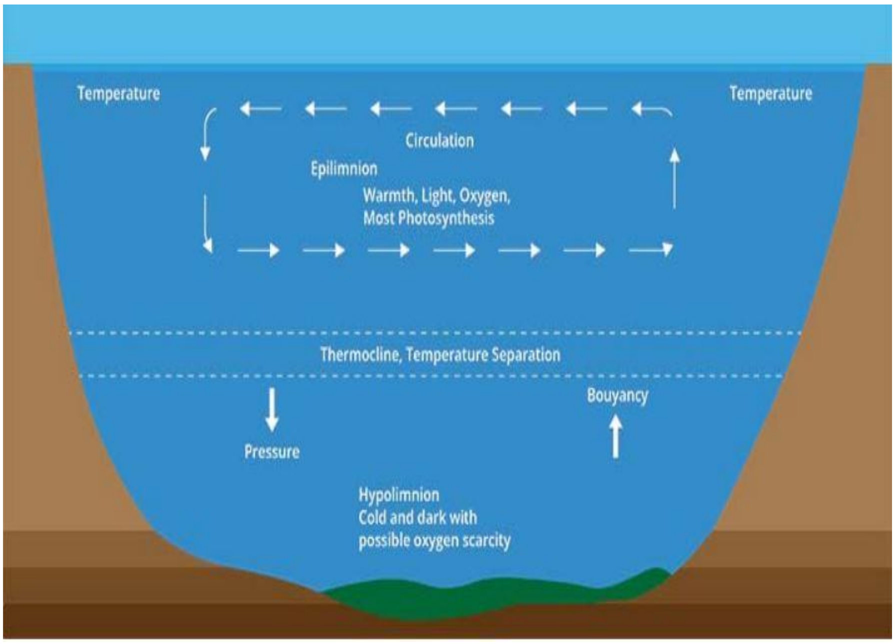

Figure 7: Water stratification [64]

Recent technology has been developed for water circulation, known as the Solar bee. This is a floating solar-powered, long-distance water circulation equipment that has been used to improve water quality in freshwater lakes, reservoirs and estuarine environments [65]. Algae usually require warm waters, high nutrient availability, sunlight and quiescent water. The Solar bee unit floats on top of the water reservoir and controls algae growth by epilimnetic circulation. The Solar bee draws water up within the epilimnion from below the surface, through an intake hose, and spreads it across the surface in a near-laminar long-distance-flow pattern as shown in Figure 8 below:

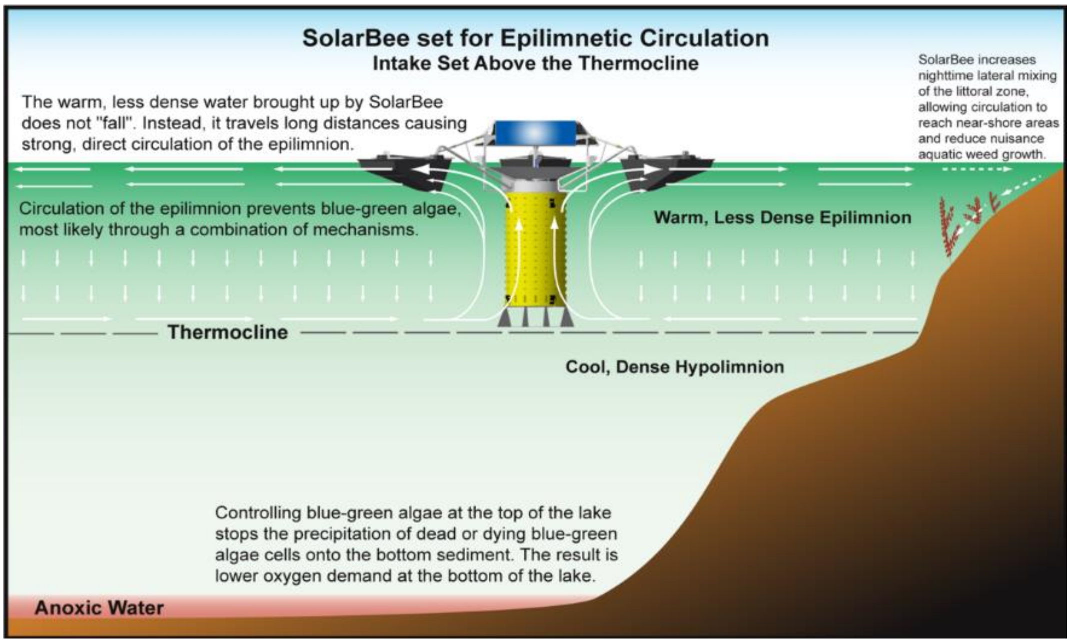

Figure 8: Solar bee for algal bloom control **[66]**

Circulation only occurs in the epilimnion layer so as to reduce the probability of bringing up the anoxic nutrient rich hypolimnetic bottom layer from beneath the thermocline. Disturbance of the nutrient-rich hypolimnetic layer can promote algal bloom in the surface waters, particularly if there is insufficient water circulation throughout the epilimnion [66]. Overall the horizontal and vertical mixing sufficiently disrupts the algaes' preferred quiescent habitat and prevents the formation of blooms.

ii. Ultrasonication

Ultrasonication is a method of applying ultrasound waves to agitate particles in a sample. For algae control in a water reservoir, ultrasounds are generated by a transducer placed in water, which floats on the water surface; and is powered by solar cells [67]. Ultrasound is a high-frequency sound wave (>20,000 Hz) above the audible frequency range of humans. The effects of ultrasound on plant cells and tissues can be mechanical or thermal in nature. When plants absorb ultrasonic waves, the energy associated with the wave is converted into heat, causing a "thermal" effect through a process known as acoustic cavitation [67]. Acoustic cavitation is a phenomenon where high power ultrasound causes the formation of bubbles that implode upon themselves causing intense heat (4,500 – 7,500 ^{0}C) and pressure (approximately 2,000 bar) [68]. Studies reveal that the heat and pressure formed cause disruption or collapse of gas vesicles and subsequent loss of buoyancy, destruction of cell membranes and cellular organelles [69]. The loss of buoyancy makes the algae sink to the bottom where there is no adequate light thus inhibiting photosynthesis and resulting in the death of the algae.

2.7.1.4 Biological methods

i. Biomanipulation

This technique involves the deliberate exploitation of the interactions between the components of the aquatic ecosystem in order to reduce algal blooms [70]. Cladoceran species such as Daphnia are effective grazers on phytoplankton, and they play an important role in improving water quality by suppressing the growth of phytoplankton populations. Biomanipulation is achieved by directly removing zooplanktivorous fish, thus manipulating fish populations to favour those that selectively consume large cladoceran species. An alternative technique is the use of piscivorous fish species. The application of fish removal and introduction during biomanipulation procedures is often limited due to the reduction in the diversity of local fish communities as this potentially leads to undesirable consequences for biodiversity and conservation [71]. Furthermore, if nutrient load remains high, biomanipulation cannot completely eradicate the effects of eutrophication.

ii. Macrophytes

Macrophytic vegetation plays an important role in maintaining the ecosystem of a water reservoir. Macrophytes are rooted plants and hence have the capacity of absorbing nutrients from the water and hence reduce the nutrient load. With the reduction of nutrient load, the rate of formation of algal blooms is also reduced [72].

2.7.2 Application of Ag-NPs for the control and inhibition of algae growth

The control and management of algal blooms are important and thus there is a great need for the introduction of efficient methods that minimize detrimental ecological and human health impacts of toxic algal blooms such as Cyanobacterial blooms. Due to the antimicrobial properties of Ag-NPs as explained in section 2.5.2, Ag-NPs can be used for the control of algal blooms. Studies have shown that the nano-sized silver particles contributes to the strong antimicrobial effect because of the high specific surface area [73].

2.7.3 Disinfection methods used in wastewater treatment

For this study, disinfection was the wastewater treatment method focused on as it is one of the most important processes for producing safe drinking water. Disinfection is carried out to deactivate pathogenic microorganisms. The various disinfection methods are described below.

1. Physical methods

i. Ultraviolet radiation

Microorganisms are inactivated by Ultra Violet (UV) light as a result of damage to nucleic acids resulting in the inability of microorganisms to grow or reproduce. Generally, this method is highly effective for protozoa, bacteria and most viruses and particularly Cryptosporidium. The high energy associated with UV light, primarily at a wavelength of 254 nm, is absorbed by cellular Ribonucleic Acid and Deoxyribonucleic Acid. UV radiation does not result in significant by-product implications. However, it is less effective for viruses than chlorine is and thus not suitable as a residual disinfectant for distribution systems [74].

ii. Membranes

Membranes act as size selective barriers, allowing some constituents to pass through the membrane and blocking the passage of others. The movement of substances across a membrane requires a driving force (potential difference across the membrane). There are four categories of pressure driven membrane processes and vary according to pore size: microfiltration (approximately 0.03 to 10 microns), ultrafiltration (0.002 to 0.1 microns), nanofiltration (0.001 microns) and reverse osmosis (0.0001 microns). Reverse osmosis and nanofiltration are typically used for the removal of both inorganic and organic compounds. Membrane filters are used for removal of bacteria, microorganisms, particulates, and natural organic material, which impart colour, tastes, and odours to water and react with disinfectants to form DBPs [75]. The substances removed or are allowed passage by different types of membrane filters are shown in Figure 9 below.

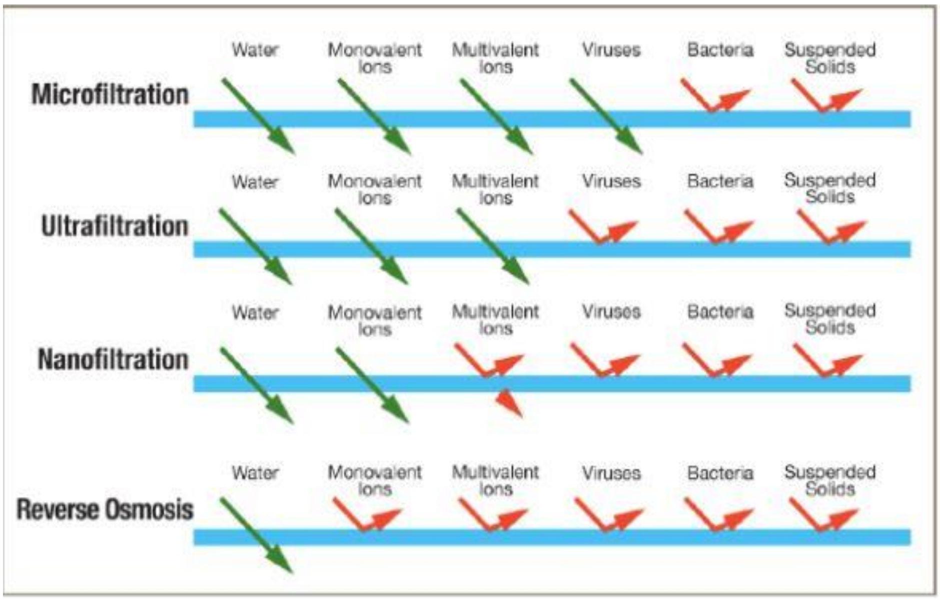

***Figure 9: Substances removed from water by membrane filtration processes* [76]**

The disadvantage of membrane filtration is that there is potential for bacterial regrowth and the contamination of water in the distribution system due to the lack of residual disinfection.

2. Chemical methods

Chemical methods depend mostly on selected chemicals with oxidizing and biocidal properties. The most commonly used disinfectants are explained below.

i. Chlorine

Chlorine is commonly used as a potable water disinfectant for both primary disinfection of treated water and for residual disinfection in distribution systems. The residual disinfection in the distribution systems ensures that the microbiological compliance is assured to the consumer tap as well as safeguarding against recontamination in the distribution system [77]. Chlorine is also commonly used in the oxidation and removal of iron and manganese. The major drawback of chlorine is that it reacts with natural organic matter such as humic substances to form DBPs. Trihalomethanes (THMs) and haloacetic acids (HAAs) are the major DBPs detected in chlorinated water. THMs include chloroform ($CHCl$), bromodichloromethane ($CHCl_2Br$), chlorodibromomethane ($CHBr_2Cl$), and bromoform ($CHBr_3$). HAAs principal components are monochloroacetic, dichloroacetic acid and trichloroacetic acid, monobromoacetic acid, dibromoacetic acid and bromochloroacetic acid. DBPs are regulated because they are considered to be potentially carcinogenic [74].

ii. Chloramine

Monochloroamine is used as a water disinfectant as it has the advantage of producing fewer DBPs as compared to chlorine and is generally stable. The disadvantage of monochloroamine is, it is a weaker and slower acting disinfectant than free chlorine. Therefore the use of monochloroamine is mainly for residual disinfection in water distribution systems to minimize the regrowth of coliforms. However, monochloroamines begin to degrade (autodecompose) to form nitrates, as a result of water age and physical conditions, such as temperature and pH in distribution systems, water is thus closely monitored [78].

iii. Chlorine dioxide

Chlorine dioxide is highly effective towards inactivation of Giardia cysts than free chlorine but less effective towards Rotavirus and *Escherichia* coli. Unlike chloramine, the disinfection efficiency of chlorine dioxide is independent of pH and the presence of ammonia. Chlorine dioxide has the advantage that it does not form significant levels of THMs. In addition, it does not react with ammonia to form chloramines. DBPs of chlorine dioxide have been identified as chlorides, chlorates and chlorites [79].

iv. Ozone

Ozone (O_3) is the most effective disinfectant for all types of microorganisms and does not result in tastes or odours after treatment. It is a powerful oxidant that reacts rapidly with most organic compounds in wastewater. Ozone lacks disinfectant residual due to rapid decomposition which results in biological regrowth problems in distribution systems. By-products of ozonation that have been identified include formaldehyde, carboxylic acids, peroxides and bromate ions [74],[79].

v. Hydrogen peroxide

Hydrogen peroxide (H_2O_2) is a strong oxidizing agent. The use of H_2O_2 in the treatment of potable water is however very limited due to its instability during storage. H_2O_2 works best through advanced oxidation processes, by the production of very reactive hydroxyl radicals through UV/O_3, O_3/H_2O_2, UV/H_2O_2 combinations or the photo Fenton reaction (UV/H_2O_2/Fe^{2+}) [80]. The hydroxyl ions are able to oxidise natural organic carbon and organic compounds. Due to high reactivity, H_2O_2 does not maintain a measurable residual level for disinfection in distribution systems thus it is not desirable.

2.7.4 Application of silver nanoparticles as a disinfectant in wastewater treatment

Prolonged use of commercial disinfectants has led to the development of resistance by some pathogens such as *Giardia* and *Cryptosporidium*. Hence, the need for re-evaluation of conventional disinfection methods. Unlike commercial disinfectants, nanoparticles do not generate harmful DBPs as they are not strong oxidants and are relatively inert. Due to the antimicrobial nature of silver as described in section 2.5.2, Ag-NPs can be applied in water treatment for disinfection purposes [81].

Currently, Ag-NPs are being applied to point-of-use water disinfection systems and anti-biofouling surfaces. The antimicrobial effect of Ag-NPs is based on the continuous release of silver ions. However, compared with Titanium dioxide, that requires energy, consuming UV light for activation, Ag-NPs kill bacteria with no need for additional energy. This makes Ag-NPs a favourable disinfectant [82]. Studies on the toxicity of Ag-NPs against microorganisms, such as *Staphylococcus aureus*, *Escherichia coli*, *Bacillus subtilis*, and *Pseudomonas aeruginosa* have been reported [83]. These have shown that Ag-NPs can be used as an effective disinfectant in water treatment.

2.8 Eco-toxicological effects of nanoparticles

Nanomaterials such as metal nanoparticles in water may not directly affect humans, but there is a possibility of uptake of nanoparticles via consumption of fish. The impact of nanomaterials on aquatic organisms thus needs to be taken into consideration. In a study reported by the US Environmental Protection Agency. The report reveals that Titanium dioxide (TiO_2) nanoparticles had an effect on aquatic organisms, including bacteria, algae, invertebrates, fish, and plants. The effects included, decreased reproduction of daphnia as well as respiratory distress, pathological changes in the gills and intestine, and behavioural changes in fish [84]. In plants, fungi and algae, Imahori [85] suggests that photosynthetic or respiratory processes are impacted as a consequence of nanoparticles penetrating the cell wall and the membrane, and reaching the cytosol.

2.9 Methods of removal of nanoparticles during water treatment

The advent of the industrial revolution has resulted in a significant increase in the use of nanoparticles. Metal nanoparticles have found use in various industries such as use in agricultural applications and consumer products. Due to the wide spread use it is expected that nanoparticles will find their way into aquatic environments [86]. Removal of nanoparticles during water treatment is an active area of research. Removal of nanoparticles during water treatment involves coagulation and flocculation to agglomerate the nanoparticles by destabilisation of their surface charge ratio and then allowing them to settle and be removed by classical filtration [87]. Magnetic nanoparticles have been made containing magnetic iron oxides, like magnetite (Fe_3O_4) and maghemite (γ-Fe_2O_3) are due to their superparamagnetism [88]. A study by Seo [89] indicates the use of a magnetically recoverable TiO_2 nanoparticle photocatalyst be easily re-collected after use during water treatment by application of a magnetic force.

2.10 Application of silver nanoparticles in catalysis

Catalysts play a very important role in chemical manufacturing processes as they improve reaction yields and reduce temperatures during fine chemical synthesis [2]. Nanoparticles possess high surface to volume ratio and a large number of active sites on the surface which play a significant role for catalytic properties [2]. Silver oxide nanoparticles are considered excellent catalysts for many catalytic reactions such as formaldehyde synthesis, nitrogen oxide (NO_x) abatement, ethylene epoxidation, oxidative coupling of methane, selective oxidation of ammonia and ethylene glycol, partial oxidation of benzyl alcohol and oxidation of styrene and carbon monoxide [90]. Ag-NPs have also been investigated to be highly active for the catalytic reduction of organic dyes such as 4-nitrophenol, methyl orange, congo red and methylene blue organic dyes present in wastewater [91].

2.11 Synthesis methods of benzaldehyde

Catalytic oxidation of alcohols to the corresponding carbonyl compounds is of significant importance in the area of fine chemicals and pharmaceutical industries. Oxidation reactions can be carried out with many different oxidants. Commonly, traditional alcohol oxidation employs the strongest stoichiometric oxidizing agents, such as pyridinium chlorochromate (PCC), pyridinium dichromate (PDC), potassium permanganate ($KMnO_4$), manganese (IV) oxide (MnO_2), sodium dichromate ($Na_2Cr_2O_7$), tetramethylpiperidine 1- oxyl (TEMPO) and chromium trioxide (CrO_3), but these oxidants are expensive, and produce hazardous by-products [92]. The conventional routes for the synthesis of benzaldehyde include hydrolysis of benzal chloride and the liquid phase oxidation of toluene using a phase transfer catalyst. In the former process, traces of chlorine inevitably exist in the product (benzaldehyde). In the latter, there is a low percentage yield as benzaldehyde is easily oxidised to benzoic acid [93].

In order to meet practical requirements of chlorine-free benzaldehyde for cosmetic, food and pharmaceutical industries, vapour phase oxidation of benzyl alcohol has been extensively investigated using catalysts such as silver-containing hexagonal mesoporous silica, mesoporous ternary metal oxide (K-Cu-TiO_2), silver/nickel (Ag/Ni) fibre, nanoporous gold, supported silver catalysts, bimetallic gold-copper catalyst and gold nanoparticles supported on mesoporous titania [94]. The limitation of vapour phase oxidation is the loss of carbon due to total oxidation of a part of benzyl alcohol into carbon dioxide at high temperature [95]. The high reaction temperature also favours energy consumption, low selectivity, and deactivation of active sites of the catalyst. Therefore, the liquid phase oxidation of benzyl alcohol at low reaction temperature is more convenient for industrial processes [96].

2.12 Uses of benzaldehyde

Benzaldehyde possesses a unique sweet, aromatic note, reminiscent of the taste and odour of almonds. It is the simplest aromatic aldehyde, widely applied in fine chemical synthesis. Benzaldehyde is a building block in the synthesis of fragrances like rose and jasmine, which are used in soaps and perfumes. Benzaldehyde is used for the production of pharmaceuticals such as pseudoephedrine, the active ingredient in most cough syrups. Benzaldehyde is further used as a building block for a range of amino acids like phenyl glycine that is used as a side chain in various antibiotics. It is also used in a wide range of insecticides such as pyrethroids and in the resin industry as a solvent, plasticizer and a low-temperature lubricant [97].

CHAPTER 3: METHODOLOGY

3.1 Introduction

This chapter gives precise details on the experimental work was carried out. The work, involved the green synthesis of Ag-NPs. The characterisation of Ag-NPs using analytical instruments. Lastly the Ag-NPs were tested for antimicrobial activity by treating algae in wastewater and catalytic activity for benzyl alcohol oxidation.

3.2 Research design

The study was of an experimental nature (field and laboratory). The field work involved the convenient non-probability sampling of freshwater algae from the Von Bach Dam and Swakop River. Laboratory work involved the green synthesis of Ag-NPs using Pearl millet husk extract as a reducing and capping agent. This was followed by characterisation of Ag-NPs using UV-Vis spectroscopy, scanning electron microscopy, transmission electron microscopy and fourier transform infra-red to identify their structural and morphological properties. The Ag-NPs were then used as an antimicrobial agent to treat algae in wastewater. The Ag-NPs were further used as a catalyst for benzyl alcohol oxidation to benzaldehyde using H_2O_2 as an oxidant.

3.3 Procedures

3.3.1 Preparation of pearl millet (*Pennisetum glaucum*) husk extract

Pearl millet grain husks were used as a source of reducing and capping agents during the synthesis of Ag-NPs. Okashana 2 pearl millet grains were obtained from Ogongo in the Omusati Region of Namibia.

i. Dehusking of pearl millet (*Pennisetum glaucum*) grains

To 10 g of pearl millet grains, approximately 100 ml of distilled water was added and allowed to soak in water for 30 minutes, then drained. The millet grains were decorticated by using a pestle and mortar to obtain husks. The husks were then separated from the grain by screening. Figure 10 below shows the pearl millet grains before decortication and figure 11 shows the pearl millet husks.

Figure 10: Pearl millet grains

Figure 11: Pearl millet husks

ii. Preparation of extract

To obtain biomolecules present in pearl millet husks, (1 g) of the husks were boiled for approximately 30 minutes in distilled water to obtain an extract. Water was used as a solvent due to its high polarity, low toxicity and would not result in the dissociation of biomolecules present in the extract [98]. The extract was cooled and filtered through a Whatman No.1 filter paper and stored in the refrigerator at 4°C for further use.

3.3.2 Synthesis of silver nanoparticles using pearl millet (Pennisetum glaucum) husk extract

The source of silver was commercially purchased silver nitrate ($AgNO_3$) from Sigma Aldrich. A typical reaction mixture contained pearl millet Extract (PME) with $AgNO_3$ solution. The synthesis was carried out in the dark to avoid the photoactivation of $AgNO_3$. The effect of PME and $AgNO_3$ concentration, pH, time and temperature parameters were studied to determine optimum conditions for Ag-NP synthesis. A blank sample containing $AgNO_3$ only was present for each experiment. The formation of Ag-NPs was observed through the colour change from colourless to orange, orange to pale brown, pale brown to brown then finally dark brown [83].

On completion of the Ag-NP synthesis, an equal volume of pure acetone was added to the Ag-NP solution to precipitate the nanoparticles. The solution was placed in a refrigerator at -15°C to allow cooling and settling of the precipitated nanoparticles overnight. The precipitated nanoparticles were separated by decanting the acetone and allowing the nanoparticles to air dry at 50°C for 20 minutes to produce a dark brown solid [99].

3.3.3 Determination of optimum conditions for Ag-NP synthesis

i. Effect of pH

To determine optimum conditions, the effect of pH was initially studied by adjusting the pH of the reaction mixtures using 1M hydrochloric acid or 1M sodium hydroxide obtained from Merck Chemicals. A pH range of 4.0 - 12.0 was used. The reaction mixture composed of 10 ml of PME and 90 ml of 1 mM $AgNO_3$ solution incubated at 50°C for 1 hour.

ii. Effect of silver nitrate concentration

After determining the optimum pH the effect of the $AgNO_3$ was determined by varying the $AgNO_3$ concentration (1.0, 1.5, 2.0, 2.5 and 3.0 mM) at the determined optimum pH and 10 ml of PME.

iii. Effect of pearl millet extract

The effect of the PME concentration was determined by varying its volume (30, 35, 40, 45 and 50 ml) while keeping the obtained optimum pH and $AgNO_3$ concentration constant.

iv. Effect of temperature

To study the effect of temperature on nanoparticle synthesis, the reaction mixtures containing the optimum concentration of PME, and $AgNO_3$ at optimum pH were incubated at 25, 50, 75 and 100°C for 1 hour.

v. Effect of time

The effect of reaction time was evaluated by incubating the reaction mixtures with optimum conditions of pH, PME, $AgNO_3$ concentration and temperature, for 20, 40, 60 minutes, 80 minutes, 100 minutes, 120 minutes, 140 minutes, 180minutes , 220 minutes and 240 minutes.

3.3.4 Characterization of the synthesized silver nanoparticles

i. Ultra Violet –Visible (UV-Vis) spectroscopy

The primary method used for the identification of Ag-NPs formed was by using a Perkin Elmer Lambda 35 UV–Vis Spectrophotometer. A characteristic SPR peak was expected in the visible range of 420- 480 nm [100]. The principle of the instrument is that, molecules absorb energy that results in translational, rotational or vibrational motion or ionization of the molecules depending upon the frequency of the electromagnetic radiation. Excited molecules are unstable and quickly drop down to the ground state giving off the received energy in the form of electromagnetic radiation. The wavelength and intensity of the electromagnetic radiation absorbed or emitted are recorded to produce a spectrum [101].

ii. Scanning electron microscopy

Scanning electron microscopy (SEM) was used to determine Ag-NPs morphology surface topography and approximate particle size using a JEOL JSM-6100 microscope. The principle of the instrument is that an electron beam is focused onto a sample surface kept in a vacuum by electromagnetic lenses. The beam is scanned over the surface of the sample and electrons scatter from the sample and are fed to a detector, and then to a cathode ray tube through an amplifier, where the images are formed, which give morphology and particle size of the sample [101].

iii. Transmission electron microscopy

Transmission electron microscopy (TEM) was used to study the morphology, topography, particle size and dispersion of nanoparticles using a JEOL JEM-1010 electron microscope. The principle of TEM is that a beam of high-energy electrons (100 – 400 keV) is collimated by magnetic lenses and allowed to pass through a sample under high vacuum. The transmitted beam and diffracted beams form a resultant diffraction pattern, which is imaged on a fluorescent screen below the sample. The diffraction pattern gives the information regarding lattice spacing and symmetry of the structure. Alternatively, the transmitted or diffracted beams can be made to form a magnified image of the sample to give information about the size and shape of the microstructural constituents of the material [101].

iv. Fourier transform – infrared spectroscopy

Fourier transform – infrared spectroscopy (FT-IR) was carried out using a Perkin Elmer spectrum 2 spectrometer to identify the possible bio-molecular interactions responsible for reduction, capping and stabilization of silver nanoparticles. The principle of the instrument is that infrared radiation is passed through a sample, which results in a higher vibrational energy of the molecule. The wavelength of light absorbed by a molecule is a function of the energy difference between the ground and excited vibrational states. The wavelengths that are absorbed by the sample are characteristic of its molecular structure [102].

3.3.5 Collection of algae

Convenience non-probability sampling was used to collect algae samples in 2 L transparent polyethylene bottles from the Von Bach dam and Swakop river. The algae samples were transferred to a wide open container and exposed to sunlight to imitate conditions in the dam in-order to preserve them.

3.3.6 Exposure of algae to silver nanoparticles

Algae was subjected to varying concentrations (2.25 mM; 3.0 mM; 3.75 mM and 4.5 mM) of Ag-NPs to determine antimicrobial effectiveness. 20 ml of algae source water was added to each sample, and the samples were exposed to sunlight to allow normal photosynthetic processes to occur. The samples were exposed to Ag-NPs for 7 days. A sample of algae without the addition of Ag-NPs was treated as a control and also exposed to sunlight for it to carry out its normal photosynthetic processes. Periodically, aliquots from algal suspensions were taken for measuring the Chlorophyll concentration using a Perkin Elmer Lambda 35 UV-Vis Spectrophotometer at range of 300 - 750 nm.

i. Visual observation

Algal death was visually observed by taking note of colour change from green to brown.

ii. Spectrophotometric determination of chlorophyll in algae

This test was carried out to measure the photosynthetic pigment present in the algae, mainly chlorophyll *a*. 1 g of algae treated with a Ag-NP solution was ground with 50 mL of 90% chilled acetone in a mortar using a pestle to extract chlorophyll. Chlorophyll extracted into the acetone solution was collected and filtered using Whatman filter paper no.1. A control (algae not treated with Ag-NP solution) was treated in the same way. The final volume of the filtrate was made up to 25 mL with

90% acetone. A Perkin Elmer Lambda 35 UV-Vis spectrophotometer was used and 80% aqueous acetone was used as a blank at 750 nm to calibrate the instrument. A cuvette was filled with the acetone chlorophyll extract and the absorbance read [103].

iii. Algal cell morphology

The genus of the algae was first identified by examining live algae under a Biomed light microscope and comparing notable cell morphology characteristics with literature. Algae was placed on a clean glass slide and a few drops of distilled water were added to improve visibility and then a clean coverslip was placed over it. After genus identification, algae samples exposed to Ag-NPs and two controls (live algae and algae that died of natural causes) were observed under the Biomed light microscope to assess cell morphology.

3.3.7 Catalytic activity of silver nanoparticles: oxidation of benzyl alcohol to benzaldehyde

i. Preparation of catalyst

Charcoal powder obtained from Merck Chemicals was used as a support for the Ag-NPs. The catalyst was prepared by doping powdered charcoal with a Ag-NP solution. 50 ml of Ag-NPs was added to 2 g charcoal powder in a round-bottomed flask. The solution was stirred using a magnetic stirrer for 20 minutes then filtered using a Buchner funnel under vacuum. The resultant Ag-NP doped charcoal was dried at 70°C and calcined at 400^0C for four hours in a furnace [16].

ii. Catalyst testing

For the catalytic oxidation of benzyl alcohol, the reaction mixture contained 30% hydrogen peroxide, 2 mM benzyl alcohol, 15 ml Acetonitrile solvent (obtained from Merck Chemicals) and 0.3 g Ag-NP doped charcoal catalyst. These were added to a round-bottomed flask, and the mixture was refluxed at 80°C and monitored by thin layer chromatography until the reaction was complete. The reaction was carried out

iii. Extraction of the crude reaction mixture

After completion of the reaction, the Ag-NP catalyst was separated from the crude reaction mixture by a simple filtration technique. The crude reaction mixture was washed by adding 10 ml of distilled water followed by extraction using 20 ml of ethyl acetate. The mixture was gently swirled and it resulted in an immiscible mixture; the bottom layer (water) and the top layer (organic product and ethyl acetate). The immiscible liquids were separated using a separating funnel. The bottom water layer was discarded. 1 g of magnesium sulphate was added to the organic product to absorb residual moisture and then filtered. The organic product containing the solvent was evaporated in a rotary evaporator to afford the crude product [104].

iv. Analysis of reaction mixture product

The organic product was analysed using a Perkin Elmer flexar high-performance liquid chromatography (HPLC) equipped with a UV-Vis detector, kinetic C18 column, column length – 250 mm, and diameter – 4 µmm, packed with 5.0 µm particles. Standard pure solutions of benzaldehyde and benzyl alcohol were analysed and their retention times compared against the retention time of the organic product obtained from the reaction mixture.

3.3.8 Energy dispersive x-ray analysis of Ag-NP doped charcoal catalyst

Energy dispersive x-ray (EDX) analysis was carried out on the Ag-NP doped charcoal catalyst to confirm doping of charcoal with Ag-NPs. EDX is used in conjunction with SEM. The principle of the instrument is that, it detects x-rays emitted from the sample during bombardment by an electron beam to characterize the elemental composition of the sample under analysis. The x-ray energy is characteristic of the element from which it was emitted [105].

3.4 Data analysis

Synthesized Ag-NPs were characterised by interpretation of spectra from UV- Vis spectroscopy, FT-IR and EDX. Micrographs from SEM and TEM were used to determine Ag-NP shape and size. Image J software was used to process and improve visual analysis of Ag-NPs to obtain the nanoparticle size. The nanoparticle size distribution was obtained through use of a histogram. Spectra from UV–Vis spectroscopy were used to determine antimicrobial effectiveness by measuring chlorophyll *a* concentration before and after treatment of algae with Ag-NPs. From the spectra obtained for chlorophyll concentration, graphs were used as a statistical analysis tool. Lastly interpretation of HPLC chromatograms was used to confirm oxidation of benzyl alcohol to benzaldehyde.

CHAPTER 4: RESULTS

4.1 Introduction

In this chapter, the results obtained for the optimization of the synthesis of Ag-NPs and characterisation of Ag-NPs according to their structural and morphological properties are presented. The antimicrobial effect of Ag-NPs on algae and catalytic activity of Ag-NPs on benzyl alcohol oxidation is also presented.

4.2 Determination of optimum conditions for Ag-NP synthesis

Formation of Ag-NPs was monitored through colour change and UV-Vis spectrum analysis of the SPR peak. The optimum condition per parameter was one that resulted in a sharp narrow SPR peak with the highest absorbance on the UV-Vis spectrum.

4.2.1 Effect of pH

The optimum pH was 10 as shown by the UV-Vis spectrum in Figure 12 below:

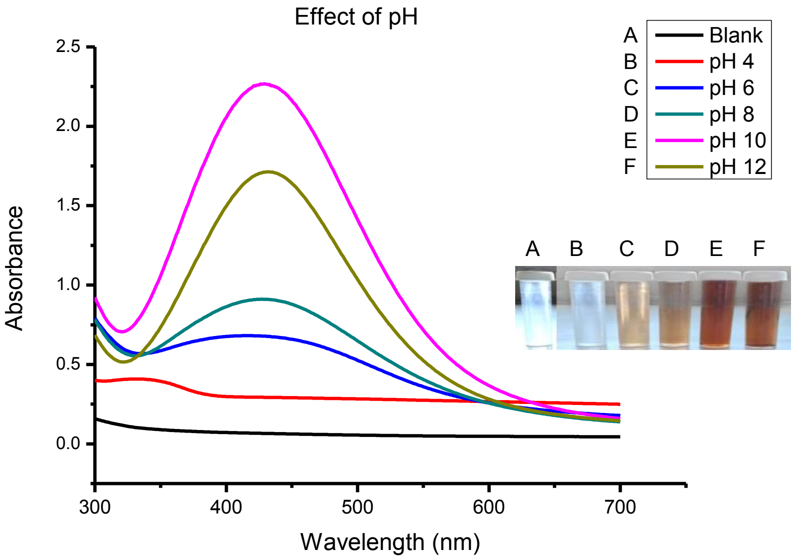

Figure 12: UV-Vis absorption spectrum of synthesized silver nanoparticles at different pH values

4.2.2 Effect of silver nitrate concentration

The optimum concentration of $AgNO_3$ was 3.0 mM as shown by the UV-Vis spectrum in Figure 13 below:

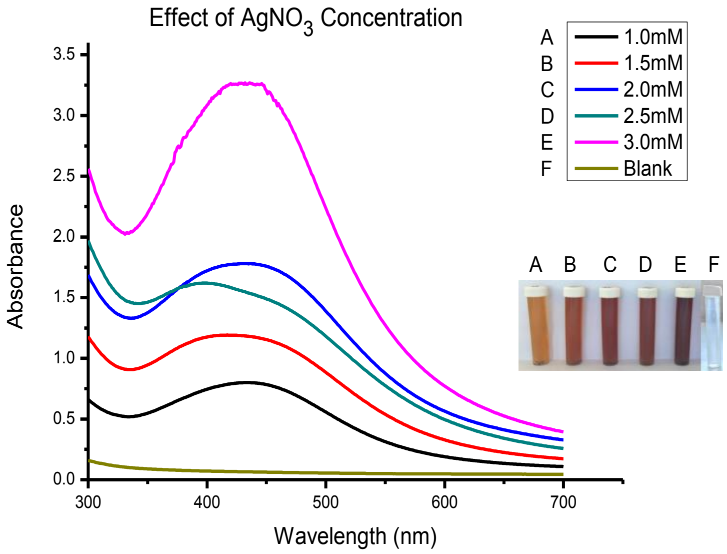

Figure 13: UV-Vis absorption spectrum of synthesized silver nanoparticles at varying $AgNO_3$ concentration

4.2.3 Effect of pearl millet extract

The optimum pearl millet extract volume was 35 ml as shown by the UV-Vis spectrum in Figure 14 below:

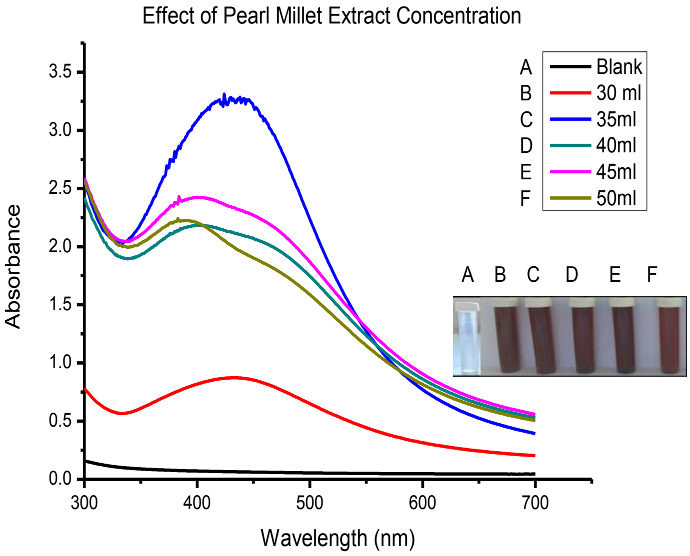

Figure 14: UV-Vis absorption spectrum of synthesized silver nanoparticles at varying Pearl Millet extract volume

4.2.4 Effect of temperature

The optimum temperature was 100^{0}C as shown by the UV-Vis spectrum in Figure 15 below:

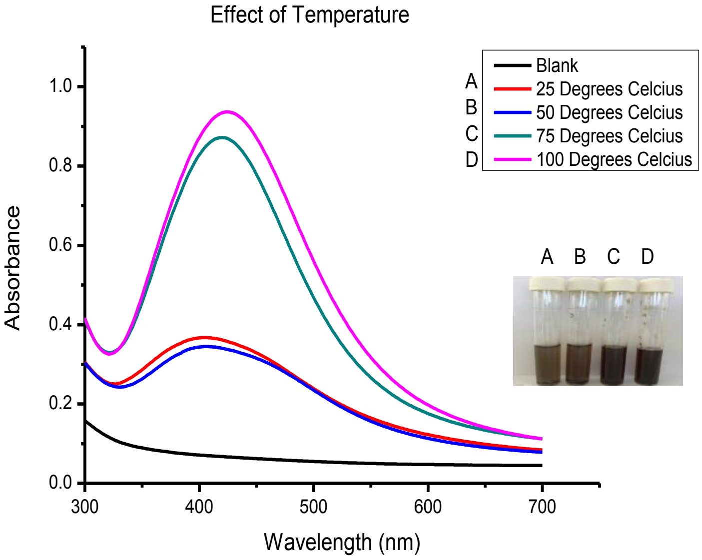

Figure 15: UV-Vis absorption spectrum of synthesized silver nanoparticles at different temperatures

4.2.5 Effect of time

The optimum reaction time was 3 hours as shown by the UV-Vis spectrum in Figure 16 below:

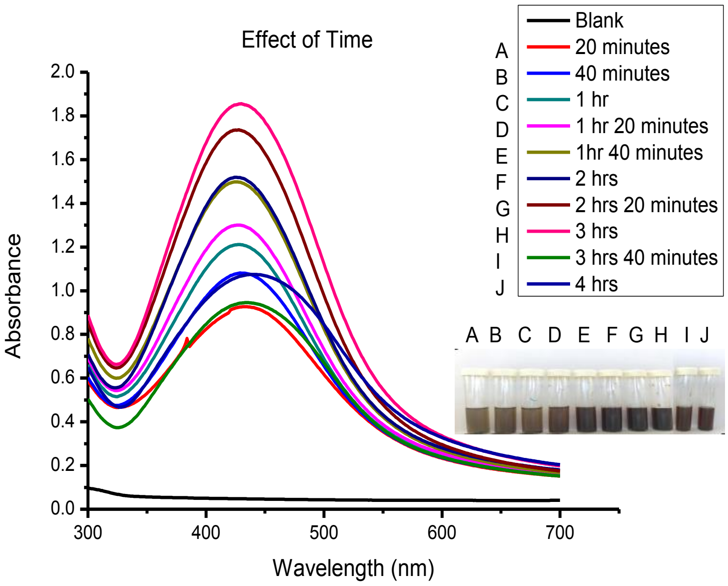

Figure 16: UV-Vis absorption spectrum of synthesized silver nanoparticles at different times

4.3 Characterisation of Ag-NPs

Ag-NPs were characterised in order to establish their optical, structural and morphological properties.

4.3.1 Absorption spectra of Ag-NPs using UV-Vis spectroscopy

UV-Vis spectroscopy was used to analyse optical properties of Ag-NPs synthesized at optimum conditions. Figure 17 below shows the SPR peak of Ag-NPs at a wavelength of 429 nm.

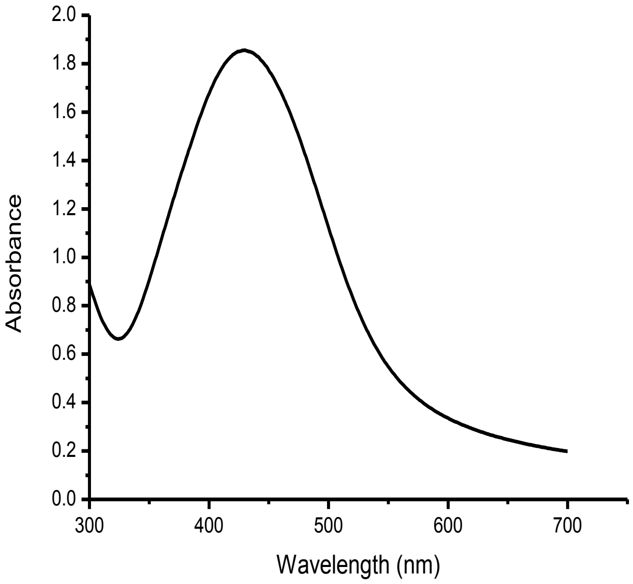

Figure 17: UV-Vis absorption spectrum of silver nanoparticles showing the SPR peak

4.3.2 FT-IR analysis

FT-IR analysis was carried out to identify the possible biomolecule functional groups present in the Pearl millet husk extract responsible for reduction, capping and stabilization of Ag^+ ions. The spectrum for the Pearl millet husk and Ag-NPs is shown in Figure 18 below:

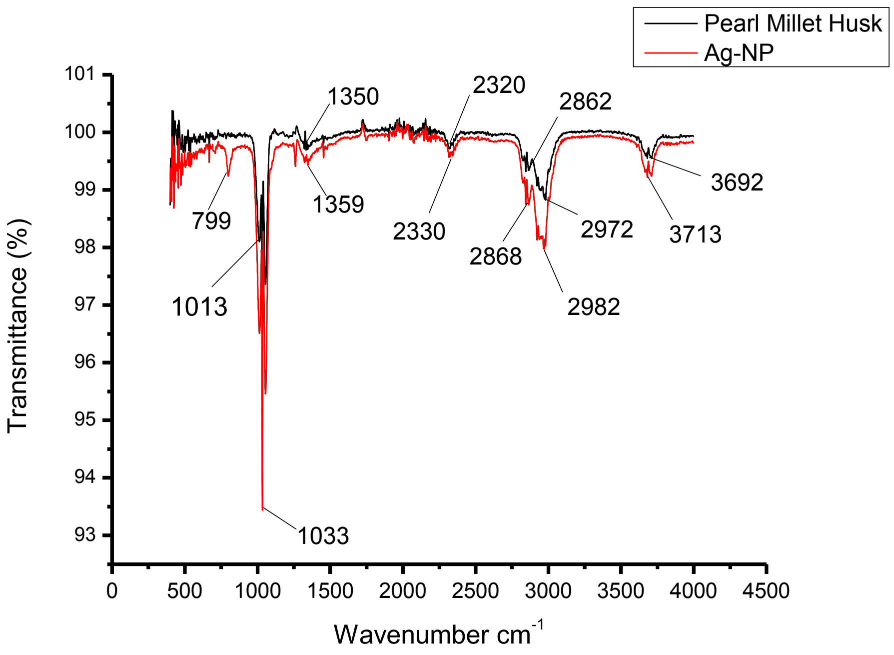

Figure 18: FT-IR spectrum of pearl millet husk and Ag-NPs

4.3.3 Morphology of Ag-NPs using TEM

TEM was used to determine the particle size, shape and dispersion of Ag-NPs. TEM micrographs are shown in Figure 19 below. Figure 20 shows the nanoparticle size distribution.

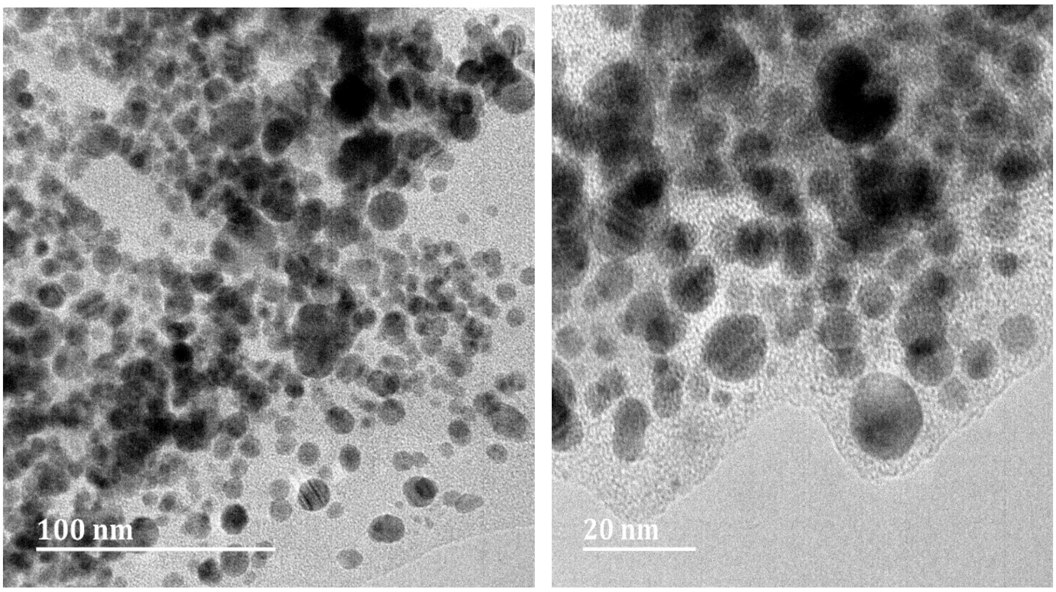

Figure 19: TEM micrographs of Ag-NPs at 100 nm and 20 nm magnification

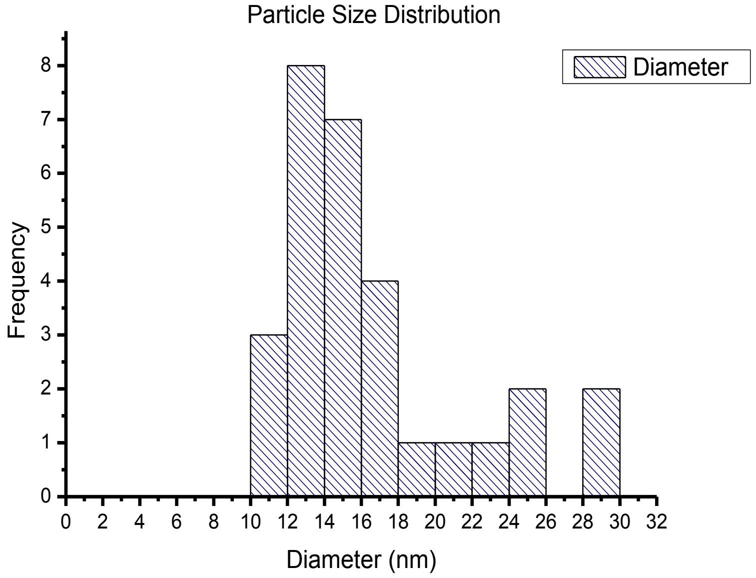

Figure 20: Particle size distribution of Ag-NPs

4.3.4 Morphology of Ag-NPs using SEM

SEM was used to determine the morphology of Ag-NPs. The SEM micrographs with a magnification of 100X and 10.00 K X respectively, are shown in Figure 21 below:

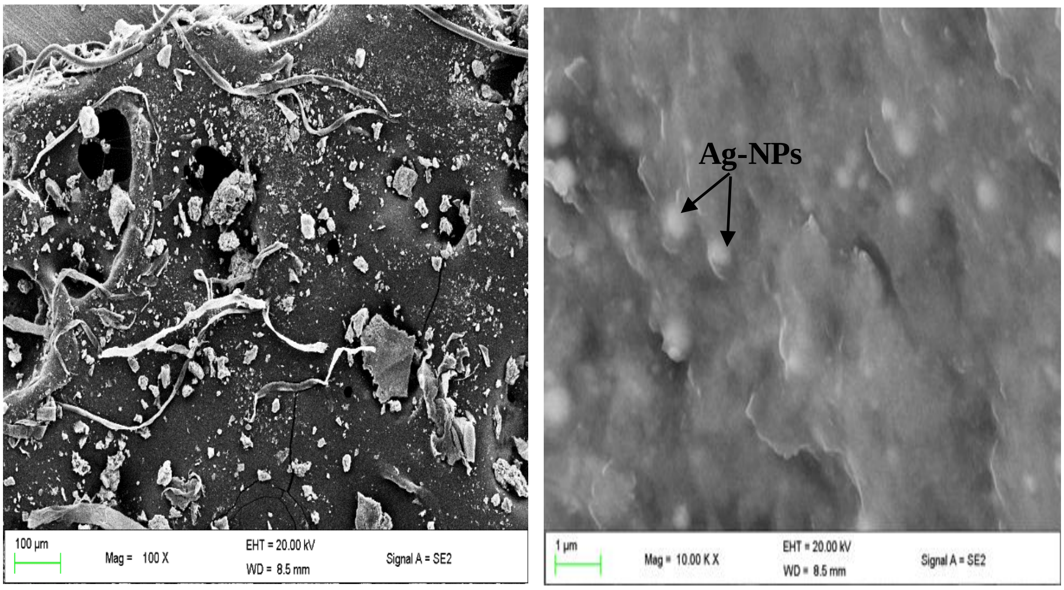

Figure 21: SEM micrographs showing the morphology of Ag-NPs

4.3.5 Morphology of Ag-NP doped charcoal catalyst using SEM

SEM was used to determine Ag-NP doped charcoal morphology. The SEM micrographs with a magnification of 100X and 14.10 K X respectively, are shown in Figure 22 below:

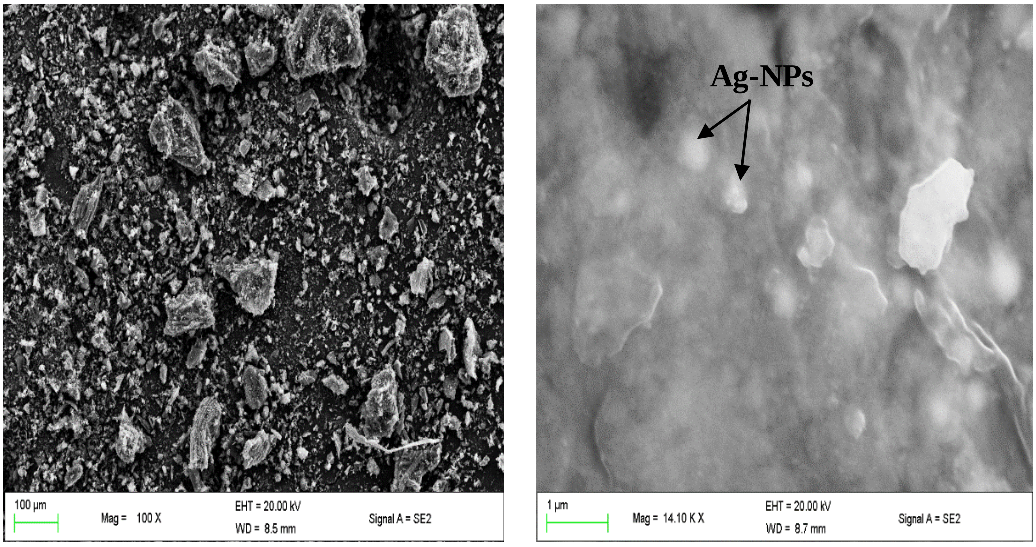

Figure 22: SEM micrographs showing the morphology of Ag-NP doped charcoal

4.3.6 Elemental analysis of Ag-NP doped charcoal catalyst using EDX

EDX analysis was carried out to confirm doping of charcoal with Ag-NPs. Figure 23 below shows the EDX spectrum of the Ag-NP doped charcoal catalyst:

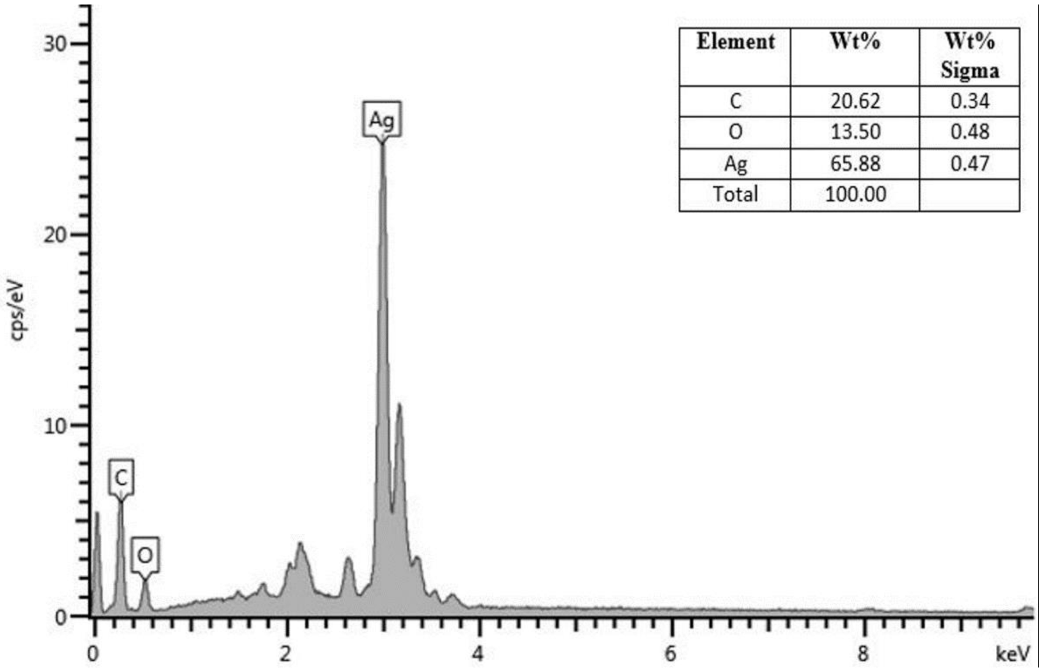

Element	Wt%	Wt% Sigma
C	20.62	0.34
O	13.50	0.48
Ag	65.88	0.47
Total	100.00	

Figure 23: EDX spectrum of Ag-NP doped charcoal catalyst

4.4 Antimicrobial activity of Ag-NPs on algae

The antimicrobial activity was studied by incubating algae in a Ag-NP solution for seven days and the chlorophyll concentration periodically analysed using UV-Vis spectroscopy.

4.4.1 Antimicrobial effect of Ag-NPs on chlorophyll concentration in algae

The graph in Figure 24 below illustrates the effect of different Ag-NP concentrations on the algae chlorophyll concentration over a period of seven days. Figure 25 shows the colour change of algae during incubation with Ag-NPs:

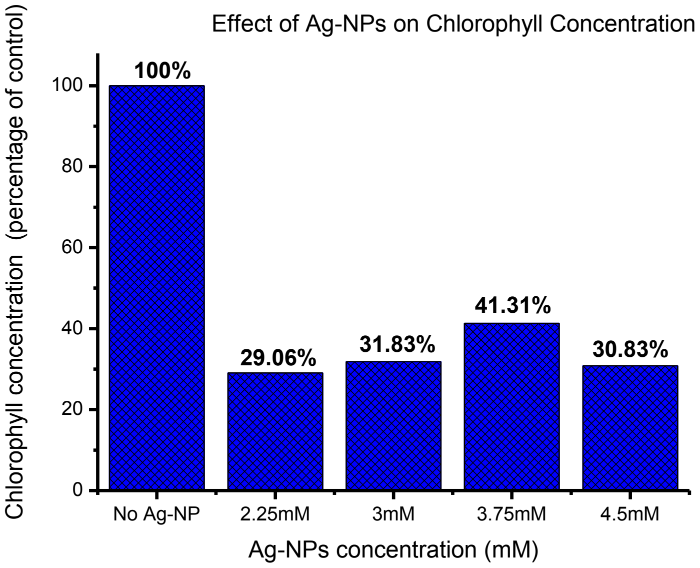

Figure 24: Variation in the chlorophyll concentration of algae upon exposure to varying Ag-NPs concentration

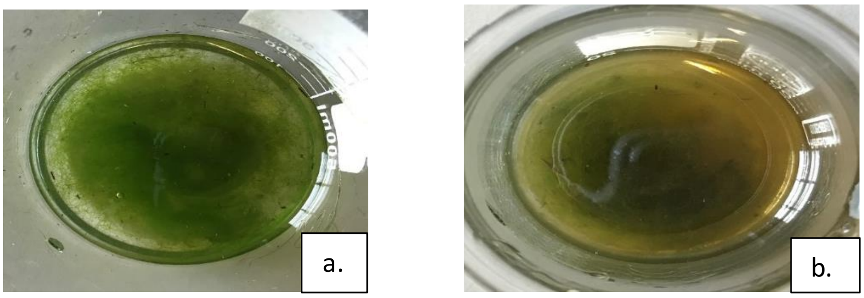

Figure 25: a. Bright green algae (control), b. Algae exposed to Ag-NPs turning dark green/brown

4.4.2 Antimicrobial effect of Ag-NPs on algae cell morphology

Algae genus was identified by comparing cell morphology of algae obtained from Von Bach dam and Swakop river to that from literature as shown in Figures 26 and 27. Cell morphology changes in algae exposed to Ag-NP solution were observed using a light microscope and compared to two controls; live and dead (death due to natural causes) algae. This is shown in Figures 27 - 29 below:

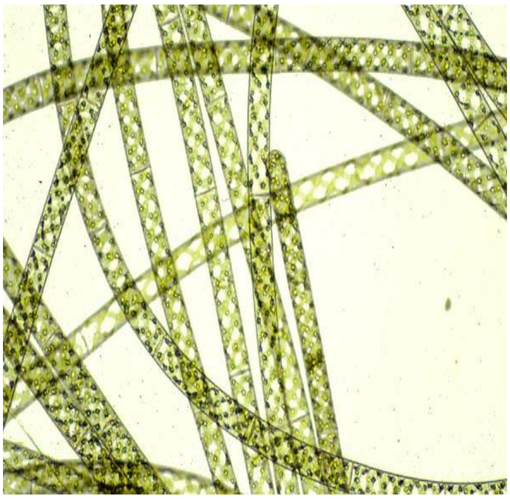

Figure 26: Live Spirogyra algae from literature [106]

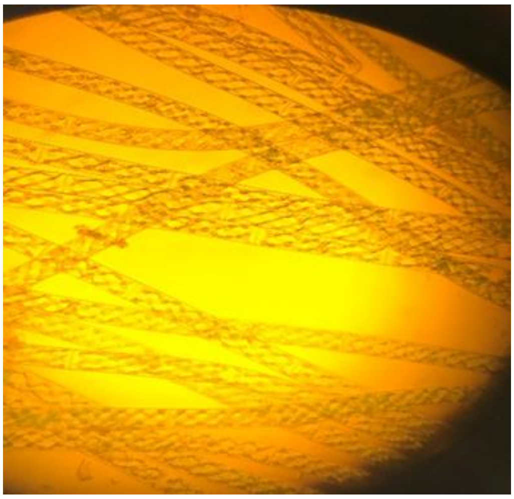

Figure 27: Live algae from Von Bach dam and Swakop river

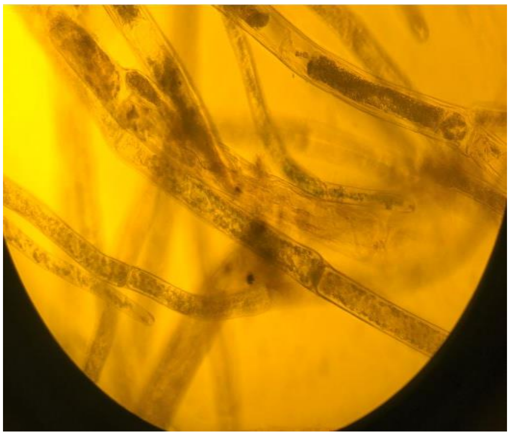

Figure 28: Dead algae (death due to natural causes)

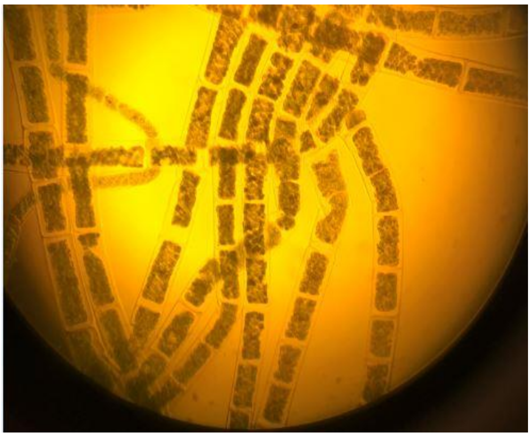

Figure 29: Dead algae exposed to Ag-NPs

4.5 Catalytic oxidation of benzyl alcohol

Benzyl alcohol was oxidised to benzaldehyde using a Ag-NP doped charcoal catalyst. The reaction mixture, standard solutions of benzyl alcohol and benzaldehyde were analysed using HPLC. Figure 30 and 31 below show the standard retention times of the starting material (pure benzyl alcohol) and the product (pure benzaldehyde) respectively. Figure 32 shows the retention time of the reaction mixture product.

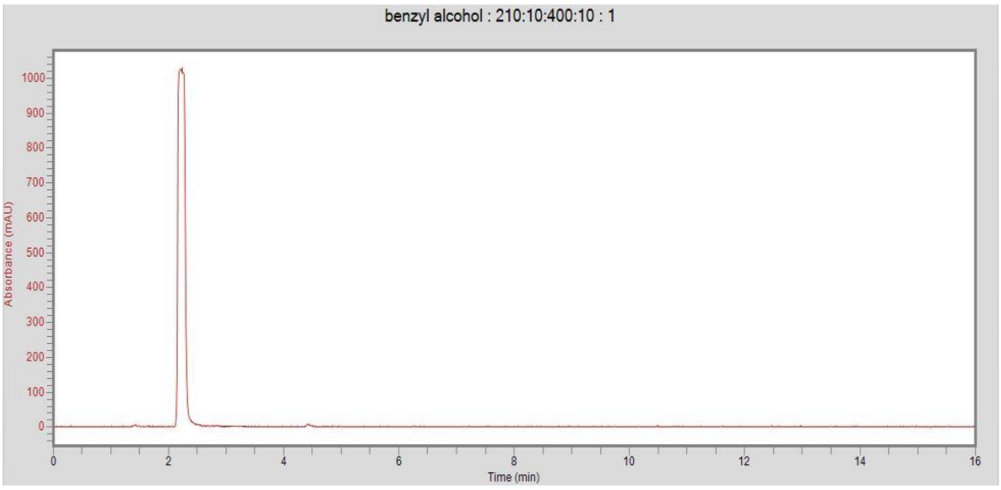

Figure 30: HPLC chromatogram showing retention time of benzyl alcohol

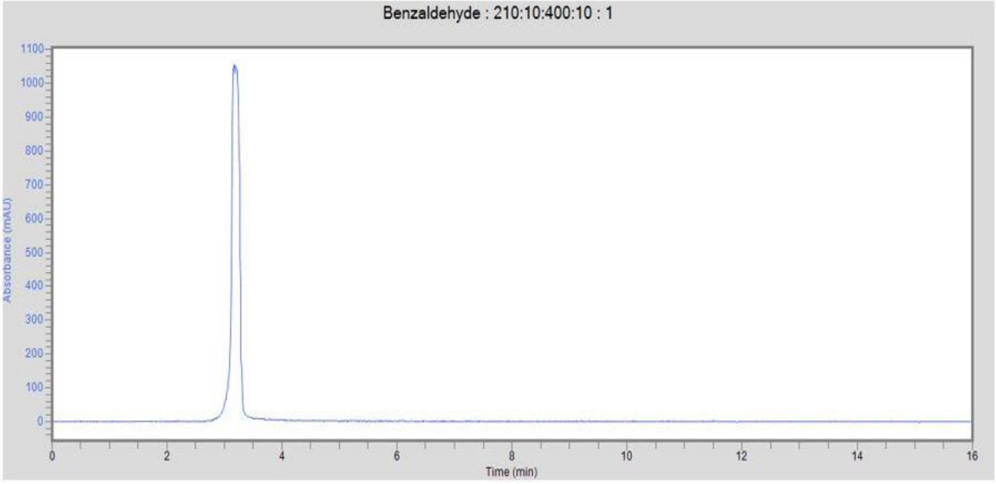

Figure 31: HPLC chromatogram showing retention time of benzaldehyde

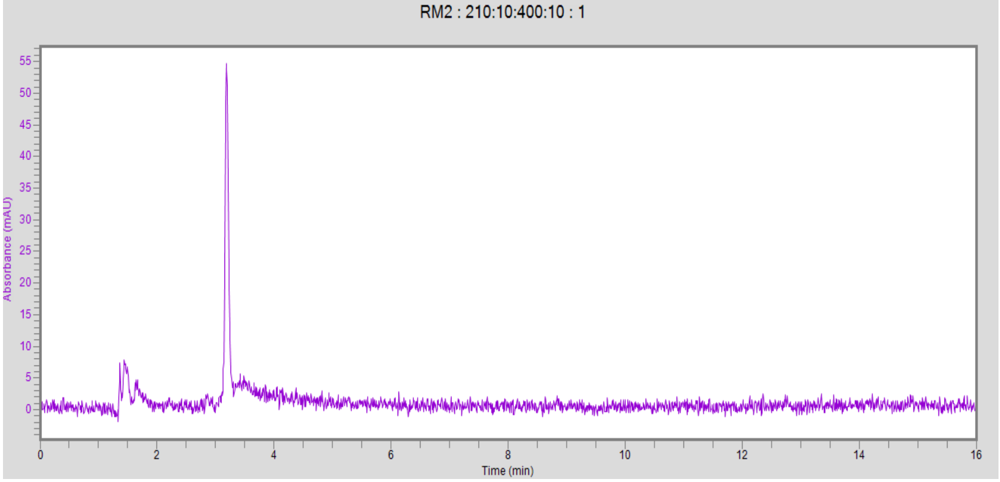

Figure 32: HPLC chromatogram showing retention time of the reaction mixture product

CHAPTER 5: DISCUSSION

5.1 Introduction

This chapter interprets the results presented in the previous chapter and intensely explains them in relation to literature.

5.2 Synthesis of silver nanoparticles

For this study Ag-NPs were synthesized using a biological method. Biosynthesis of nanoparticles is well documented, whereby plant extracts are used. Plant extracts contain biomolecules such as polysaccharides, alkaloids, phenolic acids, terpenoids, tannins, saponins, polyphenols, vitamins and proteins which play an important role in the bio-reduction of silver ions to Ag-NPs [29].

Pearl millet, the staple food of Namibia popularly known as “Mahangu” was used in this study for the synthesis of Ag-NPs. Namibian pearl millet varieties were studied by Barrion [107] and were observed to contain biomolecules such as; proteins, carbohydrates, polyphenols and C-glycosyl flavones. The available biomolecules in Pearl millet husk extract were used for reducing and stabilizing $AgNO_3$ to form Ag-NPs. Formation of Ag-NPs was visually observed by colour formation as shown in Figure 33 below. Colour formation was due to the unique optical property of surface plasmon resonance of silver, which is explained in detail in section 5.3.1.

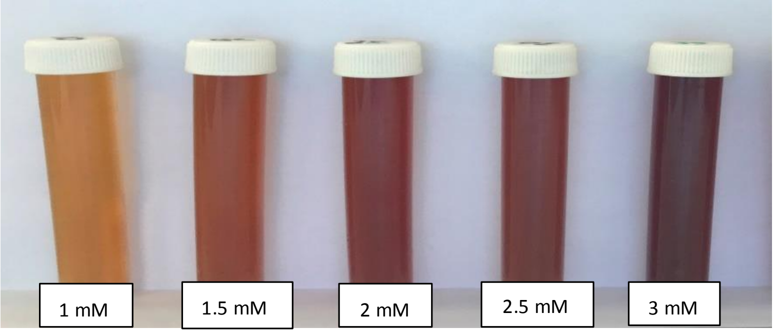

Figure 33: Colour changes during synthesis of Ag-NPs (effect of $AgNO_3$ concentration from 1- 3 mM)

5.2.1 Effect of pH

The reduction of silver ions to form Ag-NPs was dependent on the pH of the reaction mixture. As shown in Figure 12, the reaction mixture exhibited a gradual change in colour from colourless to brown with an increase in pH. This suggests that with an increase in pH there was an increase in the rate of formation of Ag-NPs. At pH 4.0, no absorption peak was observed, peak formation was observed from pH 6 onwards. Peaks sharpened and increased in absorbance with an increase in pH, however, at pH 12, low absorbance was observed. This suggests that there was reduced nanoparticle formation at very high alkaline conditions. The optimum pH was determined to be 10 as it gave the sharpest and most intense peak suggesting the highest rate of formation of nanoparticles and that alkaline conditions favour formation of nanoparticles.

In general, the reduction reaction of metallic ions is sensitive to the pH of a solution. The alkaline conditions facilitate the deprotonation of functional groups on available biomolecules. The more negatively charged biomolecules become, the more capable they are to attract more Ag^+ ions and hence increase the reduction reaction of Ag^+ ions to Ag-NPs [108]. At pH 4, no peak was observed but as conditions became more alkaline, peak formation was observed. This, therefore, indicates the necessity of hydroxyl (OH^-) ions for reduction reactions to occur for Ag-NP synthesis.

5.2.2 Effect of silver nitrate concentration

The reaction mixture of $AgNO_3$ and PME showed an increase in the colour intensity of reaction mixtures as the concentration of $AgNO_3$ increased from 1.0 mM to 3.0 mM, as shown in Figure 13. A dark brown solution was observed in the 3.0 mM $AgNO_3$ reaction mixture. Absorbance increased with increase in the $AgNO_3$ concentration, maximum absorbance was obtained at 3.0 mM $AgNO_3$ thus it was the optimum concentration. This shows that, there was an increase in the formation of Ag-NPs with an increase in $AgNO_3$ concentration. A variation in biomolecules and metal salt ($AgNO_3$) concentration influences nanoparticle synthesis. However there comes a point where there is saturation of biomolecule active sites with silver ions, and no site is available for excess ions to be reduced, hence there will be no further increase in synthesis of Ag-NPs despite the addition of more salt [109].

The silver nitrate concentration was not further increased to 3.5mM as the UV-Vis spectrum showed that aggregation was beginning to occur. When silver nanoparticles aggregate, the metal particles become electronically coupled and have a different SPR peak than the individual particles. In the case of a multi-nanoparticle aggregate, the plasmon resonance will be red-shifted to a longer wavelength than the resonance of an individual nanoparticle, and aggregation is observable as an intensity increase in the infrared region of the spectrum as shown in figure 13 [110].

5.2.3 Effect of pearl millet extract

Formation of Ag-NPs was a result of the reduction of $AgNO_3$ by available biomolecules in the PME. PME volume effect on Ag-NP formation is illustrated in Figure 14. The optimum PME volume was 35 ml as it gave the sharpest peak with the highest absorbance indicating the highest rate of formation of Ag-NPs. Further increase in the concentration of PME did not show an increase in bio-reduction of Ag^+ ions to nanoparticles as shown in Figure 14. Formation of nanoparticles was dependent on the $AgNO_3$: PME concentration ratio.

PME volume of 45 ml and 50 ml resulted in very broad peaks and a low absorbance at lower wavelengths, suggesting a blue-shift from 429 to 380 nm. The blue shift was due to a decrease in the size of the nanoparticles, this is indicative of increased capping of nanoparticles with stabilising molecules [111]. Broadening of the peak was related to the size distribution of nanoparticles. Peak broadening indicated a larger range in size or shape of particles, thus giving an overall broadening and associated decrease in the absorbance [111].

5.2.4 Effect of temperature

Figure 15 shows the effect of temperature on the synthesis of Ag-NPs. Broad peaks with low absorbance were observed for reaction mixtures at 25°C and 50°C, with SPR peaks at 400 nm. The broadening of the peaks was due to non-uniform particle size distribution as explained in section 5.2.3 above. With an increase in temperature from 50°C to 100°C, the SPR peaks became sharper indicating the formation of uniformly sized nanoparticles. The sharpest peak was observed at 100°C. The colour intensity of Ag-NP reaction mixture also increased with increase in temperature from a pale brown to a very dark brown solution. The increase in colour intensity was due to an increase in the rate of reaction thus increased formation of Ag-NPs.

The increase in the peak absorbance with an increase in temperature showed the dependence of the silver ion reduction on the reaction temperature. Upon an increase in temperature (from 50°C – 100°C), a red-shift appeared from 400 nm to 424 nm indicating an increase in Ag-NPs size [112]. As the reaction temperature increased, the reaction rate also increased, causing most Ag^+ ions to be consumed in the formation of nuclei and thus stopping the secondary reduction process on the surface of the pre-formed nuclei. Increasing the temperature beyond a certain point aids the growth of the crystal around the nucleus thus the observed increase in particle size [113]. The temperature was not further increased above 100°C as nanoparticle aggregation was beginning to occur as shown by the increase in intensity in the infrared region of the spectrum as shown in figure 15.

5.2.5 Effect of time

Figure 16 shows the effect of time on Ag-NP synthesis. It was observed that as the time progressed the SPR peak absorbance increased, this suggested continual formation of Ag-NPs with time. However, it was observed that after three hours the SPR peak decreased in absorbance and broadening occurred. The colour intensity also changed with an increase in time from pale brown to dark brown. Peak broadening was a result of a larger range in size and shape of particles with an increase in time. The change in particle size was a result of particle agglomeration nature of nanoparticles with an increase in time [114].

5.3 Characterisation of Ag-NPs

The Ag-NPs were characterised using UV-Vis Spectroscopy, FT-IR, TEM, SEM and EDX analysis.

5.3.1 Absorption spectra of Ag-NPs using UV-Vis spectroscopy

UV-Vis spectroscopy was the principal method used for the confirmation of the formation of Ag-NPs. Upon formation of Ag-NPs, orange to dark brown colours were observed as shown in Figure 33. The colours were due to unique optical properties of noble metals known as surface plasmon resonance (SPR). The SPR peak arises when there is a strong interaction of the Ag-NPs with light, this results in electrons on the metal surface to undergo a collective oscillation when excited by light at specific wavelengths [38]. The SPR peak is observed at various wavelengths in the visible region of the electromagnetic spectrum and this influences the shape of the nanoparticles. Figure 17 represents the UV-Vis analysis of Ag-NPs formed at optimum conditions of synthesis and the SPR peak was at a wavelength of 429 nm.

5.3.2 FT-IR analysis

In order to determine the functional groups of PME responsible for the reduction and stabilisation of Ag^+ ions to form Ag-NPs, FT-IR analysis was performed. Figure 18 shows a comparison between the pearl millet husk spectra and the Ag-NPs spectra. The pearl millet husk (control) spectra showed a number of peaks with different functional groups. There was a shift in the following peaks: 3692 -3713; 2972 - 2982; 2862 -2868; 2320 -2330; 1350 -1359 and 1013 -1033 cm^{-1}. The shift in the peaks indicated the involvement of the functional groups in the Ag-NP synthesis.

The peak shift at 3692 cm^{-1} was due to N–H stretching of amides or the O-H stretching vibrations of alcohols. The peak shift at 2972 cm^{-1} and 2862 cm^{-1} was due to C-H stretching of alkyls. The peak shift at 2320 cm^{-1} was due to the CN stretch of nitriles. The peak shift at 1350 cm^{-1} and 1013 cm^{-1} was due to the C-O stretch of ethers and the C=O stretch of esters respectively. This analysis provides evidence for the presence of proteins, polyphenols, flavonoids, and carbohydrates (due to functional groups of amides, hydroxyls and carbonyls). The FT-IR spectrums confirm that biomolecules in the pearl millet husk interacted with Ag^+ ions via the identified functional groups and were responsible for the reduction and stabilisation to form Ag-NPs.

5.3.3 Morphology of Ag-NPs using TEM

TEM provided insight into the morphology and exact size details of the synthesized Ag-NPs. The TEM micrographs at different magnifications showed polydispersed silver nanoparticles with a spherical shape as shown in Figure 19. Figure 20 shows that there was a variation in particle sizes of the nanoparticles. The particle sizes ranged from 10 to 30 nm with an average particle size of 17 nm.

5.3.4 Morphology of Ag-NPs using SEM

SEM was employed to analyse the structure of the nanoparticles that were formed. The micrographs as shown in Figure 21 revealed that most of the Ag-NPs were relatively spherical in shape with some irregularly shaped due to aggregation into larger particles.

5.3.5 Morphology of Ag-NP doped charcoal catalyst using SEM

The morphology of the Ag-NP doped charcoal catalyst was investigated using SEM. The micrographs are shown in Figure 22. The images reveal that most particles are of a spherical shape however not homogeneously dispersed on the surface of the charcoal.

5.3.6 Elemental analysis of Ag-NP doped charcoal catalyst using EDX

The elemental analysis of the Ag-NP doped charcoal catalyst was carried out using EDX to confirm doping of charcoal with Ag-NPs. Figure 23 shows the EDX spectrum with peaks between 3.00 - 3.40 keV corresponding to the characteristic binding energy of $Ag_{L\alpha}$, $Ag_{L\beta}$ spectral lines [115], with 11 – 26 cps/eV. Spectral lines are a series of coloured lines with dark spaces in between that occur when atoms of a specific element are emitted at a certain wavelength [116].

The peaks at binding energies of 0.3 keV and 0.5 keV were due to carbon and oxygen respectively. The carbon and oxygen were attributed to the charcoal which was used as a support for Ag-NP adsorption. According to Dimitrijević et al [117], intensities of spectral lines in EDX analysis are proportional to element abundance. Quantitative analysis showed a high silver content of 65.88% and that of carbon and oxygen at 20.62% and 13.50% respectively

5.4 Antimicrobial effect of Ag-NPs on chlorophyll concentration in algae

Chlorophyll concentration as a measure of algal growth and photosynthetic efficiency was investigated to determine the antimicrobial effect of Ag-NPs. Chlorophyll concentration in algae was reduced following exposure to Ag-NPs for an incubation period of 7 days in contrast to the control (untreated algae) as shown in Figure 24. The decrease in chlorophyll concentration was dependent on the concentration of Ag-NPs. A concentration of 3.75 mM Ag-NPs gave the highest reduction (41.31%) of chlorophyll concentration. It was also observed that the bright green coloured algae after exposure to Ag-NPs, turned dark green/brown due to progressive reduction of chlorophyll concentration as shown in Figure 25.

The reduction in chlorophyll concentration showed that Ag-NPs had a toxic effect on the algae cells. The toxicity of Ag-NPs to algae is dependent on the nanoparticles specific surface area. Cells of plants, algae, and fungi possess semi-permeable cell walls that constitute a primary site for interaction and a barrier for the entrance of some molecules into their cells. The diameter of pores across the cell wall has an average thickness of 5 to 20 nm [118]. This means that nanoparticles with a size smaller than that of the largest pore are expected to pass through the cell wall and reach the cell membrane. For this study the average nanoparticle size was determined to be 17 nm hence Ag-NPs could penetrate algae cell walls, hence the toxic effect. From the results shown in Figure 24, the Ag-NPs entered the cell and bound with organelles such as chloroplasts and pyrenoids, thus interfering with the photosynthesis processes hence the reduced chlorophyll concentration. It has also been noted that Ag-NPs in association with light alter the oxygen evolution complex, inhibit the electron transport activity as well as induce some structural deterioration thus resulting in algal death [119].

From the graph in Figure 24, with an increase in Ag-NP concentration, there was an increase in the reduction of chlorophyll concentration. However at the highest concentration of 4.5 mM, a decrease was observed, this can be explained by a phenomenon known as homo-aggregation. Homo-aggregation occurs when nanoparticles assemble into clusters due to medium composition, such as ionic strength, pH and the concentration of natural organic matter [120]. Homo-aggregation is also influenced by a high concentration of nanoparticles due to collision frequency [121]. Therefore at a concentration of 4.5 mM, some Ag-NPs homo-aggregated to form larger nanoparticles thus they could not penetrate algae cells to effectively disrupt cell activities such as photosynthesis. This, therefore, resulted in an unexpected low reduction in chlorophyll concentration.

5.5 Antimicrobial effect of Ag-NPs on algae cell morphology

The algae obtained from Von Bach dam and Swakop river (shown in Figure 27) was identified to be *Spirogyra* (Zygnematophyceae, Streptophyta) due to its filamentous nature and characteristic spiral chloroplasts after comparison with literature (shown in Figure 26). Figure 27 shows live *Spirogyra* algae obtained from the Von Bach dam and Swakop river, with cells full of cytoplasm, and the characteristic spiralling chloroplasts. Figure 29 shows *Spirogyra* algae after 7 days of exposure to Ag-NPs with cell membranes pulled away from the cell walls, and appearing to be a dense mass of shrunk cells, and the loss of the spiral chloroplast structure. The mode of Ag-NP action appeared to be by disruption of the photosynthetic function of the chloroplasts due to the loss of their spiral structure, leakage of the cytoplasm and a collapse of the cell into a dense mass and an overall loss of membrane integrity, however, no cell wall rupture was observed. Figure 28 shows *Spirogyra* algae that died due to natural causes, it shows the loss of spiral structure of the chloroplasts but however does not show the cell membrane pulling away from the cell wall to form a dense mass of shrunk cells. This, therefore, confirms that Ag-NPs were able to penetrate the algae cell membrane causing cytoplasmic damage thus the shrunken appearance as the cytoplasm is responsible for the shape of the cell. Furthermore, there was damage to the chloroplasts hence the decrease in chlorophyll concentration as explained in section 5.4 above.

5.6 Catalytic oxidation of benzyl alcohol

Benzyl alcohol was oxidised to benzaldehyde in the presence of Ag-NP doped charcoal catalyst, hydrogen peroxide and acetonitrile solvent for a total reaction time of 4 hours at 80^{o}C. HPLC was used to confirm the product of the oxidation of benzyl alcohol. Figure 30 and 31 show standard retention times of benzyl alcohol at 2.18 minutes and benzaldehyde at 3.14 minutes respectively. The retention times of the reaction mixture product was at 1.34 minutes and 3.13 minutes as shown in Figure 32. The retention time of the reaction mixture product at 3.13 minutes was not different from that obtained from the standard benzaldehyde. This suggests that the reaction mixture product was benzaldehyde.

The Ag-NP doped charcoal catalyst was able to oxidise benzyl alcohol to benzaldehyde with 90% conversion. The proposed mechanism of oxidation is shown in Figure 34 below:

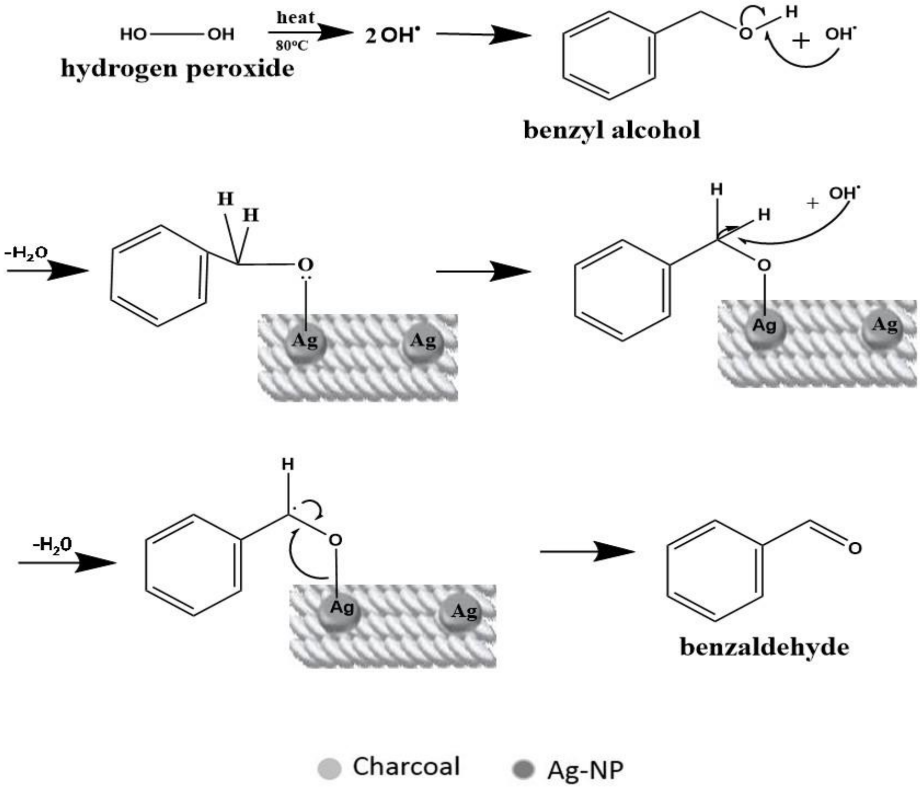

Figure 34: Proposed reaction mechanism of catalysis [16]

Essentially a catalyst creates a new reaction pathway with lower activation energy by providing a partial bond which stabilises the transition state and compensates for part of the energy required to break a bond in the reactant before stabilisation by the newly formed bond takes over [122]. For the oxidation of benzyl alcohol, the Ag-NP doped charcoal catalyst was an intermediate between benzyl alcohol and hydroxyl radicals (from hydrogen peroxide) by lowering bond dissociation energy and making electron transfer between them more efficient. The Ag-NP doped charcoal catalyst was a heterogeneous catalyst and hence was separated from the reaction mixture after reaction completion for re-use.

CHAPTER 6: CONCLUSION AND RECOMMENDATIONS

6.1: Introduction

This final chapter gives conclusions drawn from the discussions obtained from this study and gives recommendations for further study based on the experimental output.

6.2 Conclusions

In this research, Ag-NPs were successfully synthesized using pearl millet husk extract as a reducing and stabilising agent. Reaction parameters were optimised and the optimum conditions for synthesis were as follows; pH- 10, silver nitrate concentration – 3 mM, PME volume – 35 ml, temperature – 100 ^{o}C and time – 3 hours. Ag-NPs synthesized at optimum conditions were characterised. The absorption of Ag-NPs was examined using UV-Vis spectrometry and was used to control the shape and size of Ag-NPs. The SPR peak was obtained at a wavelength of 429 nm, characteristic of spherical nanoparticles. SEM and TEM analysis revealed that the Ag-NPs were spherically shaped, thus confirming the result of the SPR peak obtained. The nanoparticles were polydispersed due to some nanoparticles forming irregularly shaped aggregates. The average particle size was determined to be 17 nm. FT-IR analysis identified functional groups of biomolecules present in pearl millet husk extract to be hydroxyls, amides and carbonyls. It was therefore concluded that they belonged to proteins, polyphenols and carbohydrate biomolecules.

Ag-NPs were tested for antimicrobial activity on algae obtained from Von Bach dam and Swakop river. It was concluded that Ag-NPs at a concentration of 3.75 mM showed antimicrobial activity against algae by reducing the chlorophyll concentration by 41.31% over an incubation period of seven days. The antimicrobial activity was also evidenced by the change in morphology of algal cells by disruption of the characteristic helical structure of chloroplasts.

It was concluded that the Ag-NP doped charcoal catalyst oxidised benzyl alcohol to benzaldehyde with 90% conversion. This thus confirmed that Ag-NPs were an active catalyst for this organic transformation.

6.3 Recommendations

From the findings of this research, it is recommended that, biologically synthesized Ag-NPs, using pearl millet husk extract can be used for wastewater treatment to control algae growth and mitigating problems posed by algae blooms in water bodies. For this study, spherical shaped Ag-NPs with an average particle size of 17 nm were synthesized and tested for antimicrobial activity and were found to be toxic to algae. However further study is recommended to investigate the influence of different shapes and sizes on Ag-NPs' antimicrobial effect on algae. Furthermore, it is recommended to improve the stability of Ag-NPs to prevent aggregation during application for removal of algae during wastewater treatment. Lastly, for this study, the Ag-NP doped charcoal catalyst was calcined at 400 ^{o}C for four hours, further studies are therefore recommended to investigate the effect of different calcination temperatures and time on the catalytic activity.

REFERENCES

1. Tran QH, Nguyen VQ, Le AT. Silver nanoparticles: Synthesis, properties, toxicology, applications and perspectives. Adv Nat Sci Nanosci Nanotechnol. 2013;4(3):1–20.
2. Bhosale MA, Bhanage BM. Silver nanoparticles: Synthesis, characterization and their application as a sustainable catalyst for organic transformations. Curr Org Chem. 2015;19(8):1–20.
3. Masarovicová E, Králová K. Metal nanoparticles and plants. Ecol Chem Eng S. 2013;20(1):9–22.
4. Subbenaik SC. Physical and Chemical Nature of Nanoparticles. In: Chittaranjan K, Sakthi Kumar D, Khodakovskaya M V, editors. Plant Nanotechnology : Principles and Practices. Cham: Springer International Publishing; 2016. p. 15–28.
5. Dirkx.E, Hager.C, Tadross.M, Bethune.S, Curtis.B. Climate Change Vulnerabitlity and Adaptaiton Assessment Namibia. United Nations Development Program,. Windhoek; 2008.
6. Misra AK. Climate change and challenges of water and food security. Int J Sustain Built Environ [Internet]. 2014 Jun 1 [cited 2018 Aug 20];3(1):153–65. Available from: https://www.sciencedirect.com/science/article/pii/S221260901400020X
7. Wun Jern N. Industrial Wastewater Treatment. 1st ed. Wei TK, editor. London: Imperial College Press; 2006. 6-8 p.
8. UN Educational Scientific and Cultural Organization, UN Water. 2017 UN World Water Development Report, Wastewater_ The Untapped Resource - World _ ReliefWeb [Internet]. 2017 [cited 2017 Apr 20]. Available from:

https://reliefweb.int/report/world/2017-un-world-water-development-report-wastewater-untapped-resource

9. Pazvakawambwa GT. Water Resources Governance in the Upper Swakop Basin. University of Namibia; 2018.
10. Biggs D, Williams R. A Case Study of Intergrated Water Resource Management in Windhoek, Namibia. In: Frontiers in urban water management: Deadlock or hope? Frontières de la gestion de l 'eau urbaine: Impasse ou espoir? 2001. p. 10.
11. Garus-oas CH. Abundance and Diversity of Microalgae in Freshwater Eutrophic systems of Namibia and optimization of lipid and biomass production in Nannochloropsis Limnetica. University of Namibia; 2017.
12. Sirunda JJ. The Effects of Water Transfer from Swakoppoort and Omatako Dams on the Water Quality of Von Bach Dam, Namibia. University of the Western Cape; 2011.
13. Chislock MF, Doster E, Zitomer RA, Wilson AE. Eutrophication : Causes , Consequences , and Controls in Aquatic Ecosystems. Nat Educ Knowl. 2013;4(4):1–8.
14. Lehmann FL. Water quality of the Swakoppoort Dam, Namibia. Albert-Ludwigs University ,Freiburg, Germany; 2010.
15. Rajurkar K, Kulkarni N, Rane V, Shrivastava R. Selective Oxidation of Toluene to Benzaldehyde using Cu / Sn / Br Catalyst System. Int J Chem Sci. 2011;9(2):545–52.
16. Khan M, Syed FA, Siddiqui MRH. Nano silver-doped manganese oxide as catalyst for oxidation of benzyl alcohol and its derivatives : Synthesis, Characterisation, Thermal Study and Evaluation of Catalytic Properties. Oxid Commun 36. 2013;3(May 2014):778–791.

17. Bhushan B. Introduction to Nanotechnology. In: Handbook of Nanotechnology. 4th ed. Springer Berlin Heidelberg; 2010. p. 1–15.

18. Feynman RP. There's Plenty of Room at the Bottom. In: There's Plenty of Room at the Bottom [Internet]. 1960. p. 1–11. Available from: http://www.zyvex.com/nanotech/feynman.html

19. Calderón-jiménez B, Johnson ME, Bustos ARM, Murphy KE, Winchester MR, Baudrit JRV. Silver Nanoparticles : Technological Advances , Societal Impacts , and Metrological Challenges. Front Chem. 2017;5(6):1–26.

20. Roy S, Das TK. Plant Mediated Green Synthesis of Silver Nanoparticles-A Review. Int J Plant Biol Res. 2015;3(3):1044.

21. Mishra S. Nanotechnology in medicine. Indian Heart J. 2016;68(3):437–9.

22. Singh S, Singh B., Yadav SM, Gupta AK. Applications of nanotechnology in agricultural and their role in disease management. Res J Nanosci Nanotechnol. 2014;1–5.

23. Prasad R, Bhattacharyya A, Nguyen Q. Nanotechnology in Sustainable Agriculture: Recent Developments, Challenges, and Perspectives. Front Microb. 2017;20(8):1014.

24. National Nanotechnology Initiative. Benefits and Applications _ Nano [Internet]. [cited 2018 Aug 16]. Available from: https://www.nano.gov/you/nanotechnology-benefits

25. Boysen E. Air pollution and nanotechnology [Internet]. Vol. 1174. 2015. p. 9–11. Available from: http://www.understandingnano.com/air.html

26. Woodford C. Water Pollution [Internet]. 2017. Available from: http://www.explainthatstuff.com/waterpollution.html

27. Ahmed S, Ahmad M, Swami BL, Ikram S. A review on plants extract mediated

synthesis of silver nanoparticles for antimicrobial applications : A green expertise. J Adv Res. 2016;7(1):17–28.

28. Saravanan P, Gopalan R, Chandrasekaran V. Synthesis and Characterisation of Nanomaterials. Def Sci J. 2008;58(4):504–16.

29. Mohammadlou M, Maghsoudi H, Jafarizadeh-Malmiri H. A review on green silver nanoparticles based on plants: Synthesis, potential applications and eco-friendly approach. Int Food Res J. 2016;23(2):446–63.

30. Dhand C, Dwivedi N, Loh XJ, Jie Ying AN, Verma NK, Beuerman RW, et al. Methods and strategies for the synthesis of diverse nanoparticles and their applications: a comprehensive overview. RSC Adv [Internet]. 2015 Dec 10 [cited 2018 Sep 8];5(127):105003–37. Available from: http://xlink.rsc.org/?DOI=C5RA19388E

31. Chung I, Park I, Seung-hyun K, Thiruvengadam M, Rajakumar G. Plant-Mediated Synthesis of Silver Nanoparticles : Their Characteristic Properties and Therapeutic Applications. Nanoscale Res Lett [Internet]. 2016;11(40):1–14. Available from: http://dx.doi.org/10.1186/s11671-016-1257-4

32. Mathur M. Properties of Phtyo-Reducing Agents Utilize for Production of Nano-Particles , Existing Knowledge and Gaps. Int J Pure Appl Biosci. 2014;2(2):113–30.

33. Prasad R. Synthesis of Silver Nanoparticles in Photosynthetic Plants. J Nanoparticles [Internet]. 2014;2014:1–8. Available from: http://www.hindawi.com/journals/jnp/2014/963961/

34. Sakamoto M, Fujistuka M, Majima T. Light as a construction tool of metal nanoparticles: Synthesis and mechanism. J Photochem Photobiol C Photochem Rev [Internet]. 2009 Mar 1 [cited 2018 Sep 7];10(1):33–56. Available from:

https://www.sciencedirect.com/science/article/pii/S1389556708000865?via%3Dihub

35. Ghazali S, Noordin N. Morphology and Optical Properties of Ag-NPs: Effect of Reducing Agent to Surfactant Ratio. ARPN J Eng Appl Sci [Internet]. 2016 [cited 2018 Aug 23];11(10):6384–8. Available from: www.arpnjournals.com

36. Zhang X-F, Liu Z-G, Shen W, Gurunathan S. Silver Nanoparticles: Synthesis, Characterization, Properties, Applications, and Therapeutic Approaches. Int J Mol Sci [Internet]. 2016 Sep 13 [cited 2018 Aug 22];17(9):1–34. Available from: http://www.ncbi.nlm.nih.gov/pubmed/27649147

37. Shrivas K, Sahu S, Patra GK, Jaiswal NK, Shankar R. Localized surface plasmon resonance of silver nanoparticles for sensitive colorimetric detection of chromium in surface water, industrial waste water and vegetable samples. Anal Methods [Internet]. 2016 Feb 25 [cited 2018 Aug 22];8(9):2088–96. Available from: http://xlink.rsc.org/?DOI=C5AY03120F

38. Oldenburg SJ. Silver Nanoparticles: Properties and Applications | Sigma-Aldrich [Internet]. Sigma-Aldrick. 2017 [cited 2018 Aug 13]. Available from: http://www.sigmaaldrich.com/technical-documents/articles/materials-science/nanomaterials/silver-nanoparticles.html

39. Charles F, McKhann M., Harve J, Carlson DP., Douglas H. Oligodynamic Action Of Metallic Elements and of Metal Alloys on Certain Bacteria and Viruses. Pediatrics. 1948;2:272–89.

40. Jain RK. Copper-resistant microorganisms and their role in the environment. World J Microbiol Biotechnol. 1990;6(4):356–65.

41. Shrestha R, Joshi DR, Gopali J, Piya S. Oligodynamic Action of Silver, Copper and Brass on Enteric Bacteria Isolated from Water of Kathmandu Valley. Nepal

J Sci Technol. 2010;10(0):189–93.

42. Ngan V. Argyria [Internet]. 2005 [cited 2018 Apr 17]. Available from: https://www.dermnetnz.org/topics/argyria/

43. Seiler.C, Berendonk.T. Heavy metal driven co-selection of antibiotic resistance in soil and water bodies impacted by agriculture and aquaculture. Front Microbiol. 2012;3:1–10.

44. Duong TT, Le TS, Thu T, Tran H, Nguyen TK, Ho CT, et al. Inhibition effect of engineered silver nanoparticles to bloom forming cyanobacteria. Adv Nat Sci Nanosci Nanotechnol. 2016;7(2016):1–7.

45. Chng LL, Erathodiyil N, Ying JY. Nanostructured Catalysts for Organic Transformations. Acc Chem Res [Internet]. 2013 Aug 20 [cited 2018 Sep 6];46(8):1825–37. Available from: http://www.ncbi.nlm.nih.gov/pubmed/23350747

46. Syafiuddin A, Salmiati, Salim MR, Beng Hong Kueh A, Hadibarata T, Nur H. A Review of Silver Nanoparticles: Research Trends, Global Consumption, Synthesis, Properties, and Future Challenges. J Chinese Chem Soc. 2017;64(7):732–56.

47. Lide DR. CRC Handbook of Chemistry and Physics: A Ready-Reference Book of Chemical and Physical Data. 89th ed. New York: CRC Press; 2008.

48. Natsuki J, Hashimoto Y. A Review of Silver Nanoparticles: Synthesis Methods, Properties and Applications. Int J Mater Sci Appl [Internet]. 2015;4(5):325. Available from: http://www.sciencepublishinggroup.com/journal/paperinfo?journalid=123&doi=10.11648/j.ijmsa.20150405.17

49. Xie, L., Mäntysalo, M., Cabeyas, A. L., Feng Y, Jonsson F. Electrical

performance and reliability evaluation of inkjet-printed Ag interconnections on paper substrates. Mater Lett. 2012;88:68–72.

50. Schindler DW. Recent advances in the understanding and management of eutrophication. Am Soc Limnol Oceanogr. 2006;51:356–63.

51. Shaw GR, Moore DP, Garnett C. Eutrophication and Algal Blooms. In: Encyclopedia of Life Support Systems [Internet]. Eolss Publishers Co.Ltd; 2009 [cited 2018 Sep 13]. p. 298–327. Available from: http://www.eolss.net/sample-chapters/c06/e6-13-04-04.pdf

52. Paerl HW, Justic D. Primary Producers: Phytoplankton Ecology and Trophic Dynamics in Coastal Waters. In: Wolanski E, McLusky D, editors. Treatise on Estuarine and Coastal Science. Waltham: Academic Press; 2011. p. 23–42.

53. Burkholder JM, Anderson DM, Glibert PM. Harmful Algal Blooms and Eutrophication Nutrient Sources, Composition, and Consequences. Estuaries. 2002;25(4b):704–26.

54. Lopez CB, Dortch Q, Jewett EB. Scientific Assessment of Marine Harmful Algal Blooms [Internet]. Washington, D.C.; 2008 [cited 2018 Sep 18]. Available from: http://aquaticcommons.org/14920/1/assess_12-08.pdf

55. New Era Reporter. Saving water absolutely crucial, says NamWater as dams run dry. New Era Live [Internet]. 2016 Feb 23 [cited 2017 Sep 18]; Available from: https://neweralive.na/2016/02/23/saving-water-absolutely-crucial-namwater-dams-run-dry/

56. Water Environment Federation. Industrial Wastewater Management, Treatment, and Disposal. 3rd ed. New York: McGraw Hill; 2010. 259-290, 374-393, 424-429 p.

57. Ho L. Management Strategies for Cyanobacteria (Blue-Green Algae): A Guide

for Water Utilities. Adelaide; 2010.

58. Huh J-H, Ahn Ji-Whan. A perspective of chemical treatment for cyanobacteria control toward sustainable freshwater development. Environ Eng Res. 2017;22(1):1–11.

59. Beaulieu SE, Sengco MR, Anderson DM. Using clay to control harmful algal blooms: deposition and resuspension of clay/algal flocs. Harmful Algae. 2005;4:123–38.

60. Del Carmen Cuéllar Martínez T, Rodríguez RA, Voltolina D, Morquecho L. Effectiveness of coagulants-flocculants for removing cells and toxins of Gymnodinium catenatum. Aquaculture. 2016;452:188–93.

61. Van Oosterhout F, Lü M. The effect of phosphorus binding clay (Phoslock) in mitigating cyanobacterial nuisance: a laboratory study on the effects on water quality variables and plankton. Hydrobiologia [Internet]. 2013 [cited 2018 Sep 20];710:265–77. Available from: https://pure.knaw.nl/ws/files/486860/van_Oosterhout_&_Lurling_2013_Hydrobiologia_710_265–277.pdf

62. Bauzá L, Aguilera A, Echenique R, Andrinolo D, Giannuzzi L. Application of Hydrogen Peroxide to the Control of Eutrophic Lake Systems in Laboratory Assays. Toxins (Basel). 2014;6:2657–75.

63. Fan J. Evaluating the effectiveness of various control and water treatment processes on the membrane integrity and toxin fate of cyanobacteria [Internet]. University of Adelaide ; 2013 [cited 2018 Sep 22]. Available from: https://digital.library.adelaide.edu.au/dspace/bitstream/2440/83360/8/02whole.pdf

64. LG Sonic. Algae Control Methods to Prevent Algal Blooms [Internet]. 2018

[cited 2018 Sep 18]. Available from: https://www.lgsonic.com/blogs/algae-control/

65. Hudnell HK, Green D, Vien R, Butler S, Rahe G, Richards BA, et al. Improving wastewater mixing and oxygenation efficiency with solar-powered circulation. Clean Technol Environ Policy. 2011 Oct 11;13(5):731–42.

66. Knud-Hansen CF. Destratification in comparison to using Solar Bees for lake management [Internet]. SolarBee Inc. 2009 [cited 2018 Sep 18]. Available from: http://www.adem.state.al.us/programs/water/srfreports/DWSRFBirmingham.pdf

67. Wu M-Y, Wu J. In-vitro Investigations on Ultrasonic Control of Water Chestnut. Aquat Plant Manag. 2007;45:76–83.

68. Lowe M. Ultrasonic Control Of Algae In Stormwater Systems. In: 7th South Pacific Stormwater Conference [Internet]. Auckland: Water New Zealand; 2011 [cited 2018 Sep 20]. Available from: https://www.waternz.org.nz/Attachment?Action=Download&Attachment_id=1204

69. Zhang G , Zhang P , Wang B LH. Ultrasonic frequency effects on the removal of Microcystis aeruginosa. Ultrason Sonochem. 2006;13(5):446–50.

70. Mustapha MK. Application Of Biomanipulation In Reducing High Algal Biomass In Eutrophicated Shallow Tropical African Reservoirs. Limnetica. 2010. p. 1–7.

71. Nam GS, Lee EH, Chang KH. Application of an Algal Bloom Control Technique using Large Zooplankton Predators in An Eutrophic Agricultural Reservoir: A Preliminary Study. Irrig Drain. 2016;65(February):230–8.

72. Demeke A. Cyanobacteria blooms and biological control Methods. Int J Fauna

Biol Stud [Internet]. [cited 2018 Sep 24];2016(1):32–8. Available from: http://www.faunajournal.com/archives/2016/vol3issue1/PartA/2-6-5.pdf

73. Karumuri AK, Oswal DP, Hostetler HA, Mukhopadhyay SM. Silver nanoparticles attached to porous carbon substrates: Robust materials for chemical-free water disinfection. Mater Lett [Internet]. 2013;109:83–7. Available from: http://dx.doi.org/10.1016/j.matlet.2013.07.021

74. The Environmental Protection Agency. Water Treatment Manual : Disinfection. Wexford: Environmental Protection Agency; 2011. 31-96 p.

75. United States Protection Agency. Low-Pressure Membrane Filtration For Pathogen Removal: Application, Implementation and Regulatory Issues. 2001.

76. Safe Drinking Water Foundation. Ultrafiltration, Nanofiltration and Reverse Osmosis — Safe Drinking Water Foundation [Internet]. 2017 [cited 2018 Sep 4]. Available from: https://www.safewater.org/fact-sheets-1/2017/1/23/ultrafiltrationnanoandro

77. Environmental Protection Agency. Water Treatment Manual : Disinfection. Environmental Protection Agency, Ireland. Wexford; 2011. 1-200 p.

78. American Water Works Association. Nitrification Prevention and Control in Drinking Water. American Water Works Association. 2013.

79. World Health Organisation. Disinfectants and Disinfection By-products. In: Drinking Water Quality. p. 3–9.

80. Ebrahiem EE, Al-Maghrabi MN, Mobarki AR. Removal of organic pollutants from industrial wastewater by applying photo-Fenton oxidation technology. Arab J Chem [Internet]. 2017;10:S1674–9. Available from: http://dx.doi.org/10.1016/j.arabjc.2013.06.012

81. Prathna TC, Sharma SK, Kennedy M. Nanoparticles in household level water

treatment : An overview. Seperation Purif Technol. 2018;199(June):260–70.

82. Gehrke I, Somborn-schulz A. Innovations in nanotechnology for water treatment. Nanotechnol Sci Appl. 2015;8:1–17.

83. Ibrahim HMM. Green synthesis and characterization of silver nanoparticles using banana peel extract and their antimicrobial activity against representative microorganisms. J Radiat Res Appl Sci. 2015;8(3):265–75.

84. Davis J, Wang A, Shtakin J. Nanomaterial Case Studies: Nanoscale Titanium Dioxide in Water Treatment and in Topical Sunscreen. US EPA Res Triangle Park [Internet]. 2010;(November):13–4. Available from: http://scholar.google.com/scholar?hl=en&btnG=Search&q=intitle:Nanomaterial+Case+Studies+:+Nanoscale+Titanium+Dioxide+in+Water+Treatment+and+in+Topical+Sunscreen#0

85. Imahori H, Mori Y, Matano Y. Nanostructured artificial photosynthesis. J Photochem Photobiol C Photochem Rev. 2003;(4):51–83.

86. Navarro E, Anders AE, Ae B, Behra R, Nanna AE, Hartmann Ae B, et al. Environmental behavior and ecotoxicity of engineered nanoparticles to algae, plants, and fungi. [cited 2018 Oct 10]; Available from: https://link-springer-com.ezproxy.unam.edu.na/content/pdf/10.1007%2Fs10646-008-0214-0.pdf

87. Bizi M. Stability and flocculation of nanosilica by conventional polymer. Nat Sci. 2012;4(6):372–85.

88. Gregorio-Jauregui KM, Pineda MG, Rivera-Salinas JE, Hurtado G, Saade H, Martinez JL, et al. One-Step Method for Preparation of Magnetic Nanoparticles Coated with Chitosan. J Nanomater [Internet]. 2012 Jun 27 [cited 2019 Feb 17];2012:1–8. Available from: http://www.hindawi.com/journals/jnm/2012/813958/

89. Seo B, Lee C, Yoo D, Kofinas P, Piao Y. A magnetically recoverable photocatalyst prepared by supporting TiO 2 nanoparticles on a superparamagnetic iron oxide nanocluster core@fibrous silica shell nanocomposite. 2017 [cited 2019 Feb 17]; Available from: https://pubs.rsc.org/-/content/articlepdf/2017/ra/c6ra27907d

90. Khan IA, Sajid N, Badshah A, Wattoo MHS, Anjum DH, Nadeem MA. CO Oxidation Catalyzed by Ag Nanoparticles Supported on SnO/CeO 2. Brazilian Chem Soc. 2015;26(4):695–704.

91. Rostami-Vartooni A, Nasrollahzadeh M, Alizadeh M. Green synthesis of seashell supported silver nanoparticles using Bunium persicum seeds extract: Application of the particles for catalytic reduction of organic dyes. J Colloid Interface Sci. 2016;470:268–275.

92. He Y, Ma X, Lu M. Oxidation of alcohols with hydrogen peroxide in the presence of a new triple-site phosphotungstate. Arch Org Chem. 2012;2012(viii):187–97.

93. Lapari SS, Parham S. Oxidation of toluene and hydrogen peroxide catalyzed by Ni (II), Co (II), and Cu (II) Schiff base complexes. Int J Eng Sci Invent. 2013;2(5):62–7.

94. Opembe NN, Guild C, King'Ondu C, Nelson NC, Slowing II, Suib SL. Vapor-phase oxidation of benzyl alcohol using manganese oxide octahedral molecular sieves (OMS-2). Ind Eng Chem Res. 2014;53(49):19044–51.

95. Choudhary VR, Dumbre DK, Narkhede VS, Jana SK. Solvent-Free Selective Oxidation of Benzyl Alcohol and Benzaldehyde by tert-Butyl Hydroperoxide Using MnO- 4-Exchanged Mg–Al–Hydrotalcite Catalysts. Catal Letters [Internet]. 2003;86(4):229–33. Available from:

http://dx.doi.org/10.1023/A%3A1022620203071

96. Fan J, Dai Y, Li Y, Zheng N, Guo J, Yan X. Low-Temperature , Highly Selective , Gas-Phase Oxidation of Benzyl Alcohol over Mesoporous K-Cu-TiO 2 with Stable Copper (I) Oxidation State. Am Chem Soc. 2009;(I):15568–9.

97. Emerald Kalama Chemical. Product Information Sheet : Benzaldehyde [Internet]. [cited 2017 Feb 24]. Available from: http://www.emeraldmaterials.com/cms/kalama/page.html?p_name=Benzaldehyde

98. Interchim Inc. Solvent Properties [Internet]. 2016 [cited 2018 Oct 8]. Available from: http://www.interchiminc.com/flash-prep-hplc-solvent-properties.html

99. Sahoo PK, Kamal SSK, Kumar TJ, Sreedhar B, Singh AK, Srivastava SK. Synthesis of Silver Nanoparticles using Facile Wet Chemical Route. 2009;59(4):447–55.

100. Narasimha G, Praveen B, Mallikarjuna K, Deva Prasad Raju B. Mushrooms (Agaricus bisporus) mediated biosynthesis of sliver nanoparticles, characterization and their antimicrobial activity. Int J Nano Dimens. 2011;2:29–36.

101. SRM University. Characterization Techiques [Internet]. [cited 2018 Mar 11]. p. 19–41. Available from: http://shodhganga.inflibnet.ac.in/bitstream/10603/78994/5/chapter 2.pdf

102. Particle Analytical. FTIR [Internet]. [cited 2018 Sep 5]. Available from: http://particle.dk/methods-analytical-laboratory/ftir-identification/

103. Aminot A, Rey F. Standard procedure for the determination of chlorophyll a by spectroscopic methods. ICES Tech Mar Environ Sci [Internet].

2000;(March):25. Available from: http://www.ices.dk/ocean/procedures/timeschl.pdf

104. Zubrick JW. The Organic Chem Lab Survival Manual : A Student's Guide Techniques [Internet]. 9th ed. New Jersey: Wiley; 2012 [cited 2018 Sep 11]. 127-137 p. Available from: https://www.wiley.com/en-na/The+Organic+Chem+Lab+Survival+Manual:+A+Student's+Guide+to+Techniques,+9th+Edition-p-9781118083390

105. Materials Evaluation and Engineering. Energy Dispersive X-Ray Spectroscopy | EDS Failure Analysis | EDS Material Analysis | EDX Failure Analysis | EDX Material Analysis [Internet]. 2014 [cited 2018 Aug 23]. Available from: https://www.mee-inc.com/hamm/energy-dispersive-x-ray-spectroscopyeds/

106. Chen C, Barfuss MHJ, Pröschold T, Schagerl M. Hidden genetic diversity in the green alga Spirogyra (Zygnematophyceae, Streptophyta). BMC Evol Biol [Internet]. 2012 Jun 1 [cited 2018 Nov 9];12:77. Available from: http://www.ncbi.nlm.nih.gov/pubmed/22655677

107. Barrion SC. Pearl millet milling: Comparison between traditional Namibian fermentation- semi-wet milling and dry milling. 2008.

108. Sanghi R, Verma P. Biomimetic synthesis and characterisation of protein capped silver nanoparticles. Bioresour Technol. 2009 Jan 1;100(1):501–4.

109. Prathna TC, Chandrasekaran N, Raichur AM, Mukherjee A. Biomimetic synthesis of silver nanoparticles by Citrus limon (lemon) aqueous extract and theoretical prediction of particle size. Colloids Surfaces B Biointerfaces. 2011 Jan 1;82(1):152–9.

110. Oldenburg SJ. Silver Nanoparticles: Properties and Applications | Sigma-Aldrich. Materials Science Products. 2015.

111. Ashraf JM, Ansari MA, Khan HM, Alzohairy MA, Choi I. Green synthesis of silver nanoparticles and characterization of their inhibitory effects on AGEs formation using biophysical techniques. Sci Rep [Internet]. 2016 Feb 2 [cited 2018 Oct 9];6:20414. Available from: http://www.ncbi.nlm.nih.gov/pubmed/26829907

112. Amin M, Anwar F, Ramzan M, Ashraf S. Green Synthesis of Silver Nanoparticles through Reduction with Solanum xanthocarpum L . Berry Extract : Characterization , Antimicrobial and Urease Inhibitory Activities against Helicobacter pylori. Int J Mol Sci. 2012;13:9923–41.

113. Sun Y, Mayers B, Xia Y. Transformation of Silver Nanospheres into Nanobelts and Triangular Nanoplates through a Thermal Process. Nano Lett [Internet]. 2003 May [cited 2018 Oct 9];3(5):675–9. Available from: http://pubs.acs.org/doi/abs/10.1021/nl034140t

114. Prathna TC, Chandrasekaran N, Raichur AM, Mukherjee A. Kinetic evolution studies of silver nanoparticles in a bio-based green synthesis process. Colloids Surfaces A Physicochem Eng Asp [Internet]. 2011 Mar 5 [cited 2018 Oct 9];377(1–3):212–6. Available from: https://www.sciencedirect.com/science/article/pii/S0927775711000173?via%3Dihub

115. Guzmán M, Dille J, Godet S. Synthesis of silver nanoparticles by chemical reduction method and their antibacterial activity. Int J Chem Biomol Eng. 2009;2(3):104–111.

116. Hollas MJ. Basic Atomic and Molecular Spectroscopy. In: Tutorial Chemistry Texts. Cambridge: Royal Society of Chemistry; 2002. p. 107–9.

117. Dimitrijević R, Cvetković O, Miodragović Z, Simić M, Manojlović D, Jović V.

SEM/EDX and XRD Characterization of Silver Nanocrystalline Thin Film Prepared from Organomettalic Solution Precursor. J Min Metall Sect B Metall J Min Met Sect B-Metall [Internet]. 2013 [cited 2018 Nov 5];49(1):91–5. Available from: http://www.doiserbia.nb.rs/img/doi/1450-5339/2013/1450-53391200041D.pdf

118. Madigan MT, Martinko JM PJ. Prokaryotic Diversity: The Bacteria. In: Brock Biology of Microorganisms. 11th ed. New Jersey: Pearson Prentice Hall; 2006.

119. Oukarroum A, Bras S, Perreault F, Popovic R. Inhibitory effects of silver nanoparticles in two green algae, Chlorella vulgaris and Dunaliella tertiolecta. Ecotoxicol Environ Saf. 2012;78:80–5.

120. Schirmer K, Behra R, Sigg L, Sutter MJ-F. Ecotoxicological Aspects of Nanomaterials in the Aquatic Environment. Saf Asp Eng Nanomater [Internet]. 2013;0:141–62. Available from: http://infoscience.epfl.ch/record/197935/files/Chap-05.pdf

121. Baalousha M, Sikder M, Prasad A, Lead J, Merrifield R, Chandler GT. The concentration-dependent behaviour of nanoparticles Rapid Communication. Environ Chem [Internet]. 2016 [cited 2018 Oct 10];13:1–3. Available from: http://dx.doi.org/10.1071/EN15142JournalcompilationÓCSIRO2016www.publish.csiro.au/journals/env

122. Roduner E. Understanding Catalysis. Chem Soc Rev [Internet]. 2014 [cited 2018 Oct 11];1–33. Available from: https://pubs.rsc.org/ru/content/getauthorversionpdf/C4CS00210E

APPENDICES